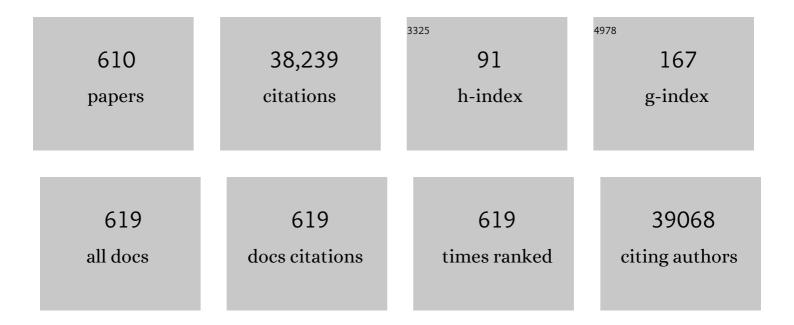
Chun-Zhong Li

List of Publications by Year in descending order

Source: https://exaly.com/author-pdf/1388003/publications.pdf Version: 2024-02-01



#	Article	IF	CITATIONS
1	Graphene quantum dots: emergent nanolights for bioimaging, sensors, catalysis and photovoltaic devices. Chemical Communications, 2012, 48, 3686.	2.2	1,845
2	3D carbon based nanostructures for advanced supercapacitors. Energy and Environmental Science, 2013, 6, 41-53.	15.6	1,389
3	Advanced Energy Storage Devices: Basic Principles, Analytical Methods, and Rational Materials Design. Advanced Science, 2018, 5, 1700322.	5.6	1,043
4	Facile preparation and upconversion luminescence of graphene quantum dots. Chemical Communications, 2011, 47, 2580-2582.	2.2	734
5	Mesoporous Carbon Incorporated Metal Oxide Nanomaterials as Supercapacitor Electrodes. Advanced Materials, 2012, 24, 4197-4202.	11.1	548
6	Hierarchical porous NiCo2O4 nanowires for high-rate supercapacitors. Chemical Communications, 2012, 48, 4465.	2.2	544
7	Preparation of graphene–TiO ₂ composites with enhanced photocatalytic activity. New Journal of Chemistry, 2011, 35, 353-359.	1.4	538
8	Cobalt nanoparticles embedded in N-doped carbon as an efficient bifunctional electrocatalyst for oxygen reduction and evolution reactions. Nanoscale, 2014, 6, 15080-15089.	2.8	509
9	2D Monolayer MoS ₂ –Carbon Interoverlapped Superstructure: Engineering Ideal Atomic Interface for Lithium Ion Storage. Advanced Materials, 2015, 27, 3687-3695.	11.1	504
10	Facile Ultrasonic Synthesis of CoO Quantum Dot/Graphene Nanosheet Composites with High Lithium Storage Capacity. ACS Nano, 2012, 6, 1074-1081.	7.3	475
11	One-pot hydrothermal synthesis of graphenequantum dots surface-passivated by polyethylene glycol and their photoelectric conversion under near-infrared light. New Journal of Chemistry, 2012, 36, 97-101.	1.4	460
12	Transition metals (Fe, Co, and Ni) encapsulated in nitrogen-doped carbon nanotubes as bi-functional catalysts for oxygen electrode reactions. Journal of Materials Chemistry A, 2016, 4, 1694-1701.	5.2	460
13	Interface Engineering of Hierarchical Branched Moâ€Doped Ni ₃ S ₂ /Ni <i>_x</i> P <i>_y</i> Hollow Heterostructure Nanorods for Efficient Overall Water Splitting. Advanced Energy Materials, 2020, 10, 1903891.	10.2	443
14	Hierarchical self-assembly of ultrathin nickel hydroxide nanoflakes for high-performance supercapacitors. Journal of Materials Chemistry, 2011, 21, 3818.	6.7	430
15	Rational Design of MnO/Carbon Nanopeapods with Internal Void Space for High-Rate and Long-Life Li-Ion Batteries. ACS Nano, 2014, 8, 6038-6046.	7.3	420
16	Heteroatom-doped carbon dots: synthesis, characterization, properties, photoluminescence mechanism and biological applications. Journal of Materials Chemistry B, 2016, 4, 7204-7219.	2.9	396
17	A novel hydrogen peroxide biosensor based on Au–graphene–HRP–chitosan biocomposites. Electrochimica Acta, 2010, 55, 3055-3060.	2.6	358
18	3D Ordered Macroporous MoS ₂ @C Nanostructure for Flexible Liâ€ion Batteries. Advanced Materials. 2017. 29. 1603020.	11.1	350

#	Article	IF	CITATIONS
19	Heterogeneous interface engineered atomic configuration on ultrathin Ni(OH)2/Ni3S2 nanoforests for efficient water splitting. Applied Catalysis B: Environmental, 2019, 242, 60-66.	10.8	332
20	High–rate electrochemical capacitors from highly graphitic carbon–tipped manganese oxide/mesoporous carbon/manganese oxide hybrid nanowires. Energy and Environmental Science, 2011, 4, 1813.	15.6	315
21	An investigation on tribological properties of graphite nanosheets as oil additive. Wear, 2006, 261, 140-144.	1.5	298
22	Carbon dots as fluorescent probes for "off–on―detection of Cu2+ and l-cysteine in aqueous solution. Biosensors and Bioelectronics, 2014, 51, 330-335.	5.3	278
23	A green and high energy density asymmetric supercapacitor based on ultrathin MnO ₂ nanostructures and functional mesoporous carbon nanotube electrodes. Nanoscale, 2012, 4, 807-812.	2.8	276
24	Synthesis of photoluminescent carbogenic dots using mesoporous silica spheres as nanoreactors. Chemical Communications, 2011, 47, 764-766.	2.2	273
25	Iron Carbide Nanoparticles Encapsulated in Mesoporous Fe–N-Doped Graphene-Like Carbon Hybrids as Efficient Bifunctional Oxygen Electrocatalysts. ACS Applied Materials & Interfaces, 2015, 7, 21511-21520.	4.0	262
26	High-performance supercapacitor material based on Ni(OH)2 nanowire-MnO2 nanoflakes core–shell nanostructures. Chemical Communications, 2012, 48, 2606.	2.2	244
27	Enriched graphitic N-doped carbon-supported Fe ₃ O ₄ nanoparticles as efficient electrocatalysts for oxygen reduction reaction. Journal of Materials Chemistry A, 2014, 2, 7281-7287.	5.2	235
28	Ultrafine manganese dioxidenanowire network for high-performance supercapacitors. Chemical Communications, 2011, 47, 1264-1266.	2.2	224
29	Synthesis and optical properties of TiO2 nanoparticles. Materials Letters, 2007, 61, 79-83.	1.3	216
30	Higher charge/discharge rates of lithium-ions across engineered TiO2 surfaces leads to enhanced battery performance. Chemical Communications, 2010, 46, 6129.	2.2	216
31	Surface-modified antibacterial TiO2/Ag+ nanoparticles: Preparation and properties. Applied Surface Science, 2006, 252, 4154-4160.	3.1	212
32	Zn-doped TiO2 nanoparticles with high photocatalytic activity synthesized by hydrogen–oxygen diffusion flame. Applied Catalysis B: Environmental, 2008, 79, 208-215.	10.8	209
33	Atomic heterointerface engineering overcomes the activity limitation of electrocatalysts and promises highly-efficient alkaline water splitting. Energy and Environmental Science, 2021, 14, 5228-5259.	15.6	198
34	2D Nanospace Confined Synthesis of Pseudocapacitanceâ€Dominated MoS ₂ â€inâ€īi ₃ C ₂ Superstructure for Ultrafast and Stable Li/Naâ€ion Batteries. Advanced Functional Materials, 2018, 28, 1804306.	7.8	194
35	Fluorination-enabled Reconstruction of NiFe Electrocatalysts for Efficient Water Oxidation. Nano Letters, 2021, 21, 492-499.	4.5	190
36	Ultra-thin anatase TiO ₂ nanosheets dominated with {001} facets: thickness-controlled synthesis, growth mechanism and water-splitting properties. CrystEngComm, 2011, 13, 1378-1383.	1.3	189

#	Article	IF	CITATIONS
37	Rapid degradation of methylene blue in a novel heterogeneous Fe3O4 @rGO@TiO2-catalyzed photo-Fenton system. Scientific Reports, 2015, 5, 10632.	1.6	186
38	Hydrothermal synthesis of novel Mn3O4 nano-octahedrons with enhanced supercapacitors performances. Nanoscale, 2010, 2, 2195.	2.8	184
39	In-situ enriching active sites on co-doped Fe-Co4N@N-C nanosheet array as air cathode for flexible rechargeable Zn-air batteries. Applied Catalysis B: Environmental, 2019, 256, 117893.	10.8	184
40	In situ assembly of graphene sheets-supported SnS2 nanoplates into 3D macroporous aerogels for high-performance lithium ion batteries. Journal of Power Sources, 2013, 237, 178-186.	4.0	182
41	Nitrogen and Phosphorus Dualâ€Doped Hierarchical Porous Carbon Foams as Efficient Metalâ€Free Electrocatalysts for Oxygen Reduction Reactions. Chemistry - A European Journal, 2014, 20, 3106-3112.	1.7	179
42	Highly efficient reusable catalyst based on silicon nanowire arrays decorated with copper nanoparticles. Journal of Materials Chemistry A, 2014, 2, 9040.	5.2	170
43	Growth of polyaniline nanowhiskers on mesoporous carbon for supercapacitor application. Journal of Power Sources, 2011, 196, 7835-7840.	4.0	166
44	Highly Stretchable Conductors Integrated with a Conductive Carbon Nanotube/Graphene Network and 3D Porous Poly(dimethylsiloxane). Advanced Functional Materials, 2014, 24, 7548-7556.	7.8	162
45	Anatase TiO ₂ Crystals with Exposed Highâ€Index Facets. Angewandte Chemie - International Edition, 2011, 50, 3764-3768.	7.2	159
46	Unsaturated Sulfur Edge Engineering of Strongly Coupled MoS ₂ Nanosheet–Carbon Macroporous Hybrid Catalyst for Enhanced Hydrogen Generation. Advanced Energy Materials, 2019, 9, 1802553.	10.2	159
47	Flame sprayed V-doped TiO2 nanoparticles with enhanced photocatalytic activity under visible light irradiation. Chemical Engineering Journal, 2009, 151, 220-227.	6.6	157
48	Hydrothermal Stability of {001} Faceted Anatase TiO ₂ . Chemistry of Materials, 2011, 23, 3486-3494.	3.2	157
49	Polyaniline–MnO2 coaxial nanofiber with hierarchical structure for high-performance supercapacitors. Journal of Materials Chemistry, 2012, 22, 16939.	6.7	157
50	Synthesis of poly(aniline-co-o-anisidine)-intercalated graphite oxide composite by delamination/reassembling method. Carbon, 2005, 43, 2564-2570.	5.4	155
51	One-pot preparation of graphene/Fe3O4 composites by a solvothermal reaction. New Journal of Chemistry, 2010, 34, 2950.	1.4	154
52	Surface enrichment and diffusion enabling gradient-doping and coating of Ni-rich cathode toward Li-ion batteries. Nature Communications, 2021, 12, 4564.	5.8	153
53	Hollow mesoporous NiCo ₂ O ₄ nanocages as efficient electrocatalysts for oxygen evolution reaction. Dalton Transactions, 2015, 44, 4148-4154.	1.6	151
54	Synthesis and optical characterization of Co3O4 nanocrystals. Journal of Crystal Growth, 2007, 304, 369-373.	0.7	149

#	Article	IF	CITATIONS
55	In situ surface hydrogenation synthesis of Ti ³⁺ self-doped TiO ₂ with enhanced visible light photoactivity. Nanoscale, 2014, 6, 9078-9084.	2.8	149
56	Electric Papers of Graphene-Coated Co ₃ O ₄ Fibers for High-Performance Lithium-Ion Batteries. ACS Applied Materials & Interfaces, 2013, 5, 997-1002.	4.0	145
57	One-step preparation, characterization and visible-light photocatalytic activity of Cr-doped TiO2 with anatase and rutile bicrystalline phases. Chemical Engineering Journal, 2012, 191, 402-409.	6.6	139
58	Room-Temperature Synthesis of Mn-Doped Cesium Lead Halide Quantum Dots with High Mn Substitution Ratio. Journal of Physical Chemistry Letters, 2017, 8, 4167-4171.	2.1	139
59	CsPbBr ₃ Perovskite Quantum Dots-Based Monolithic Electrospun Fiber Membrane as an Ultrastable and Ultrasensitive Fluorescent Sensor in Aqueous Medium. Journal of Physical Chemistry Letters, 2016, 7, 4253-4258.	2.1	137
60	Hierarchical porous nanostructures assembled from ultrathin MnO ₂ nanoflakes with enhanced supercapacitive performances. Journal of Materials Chemistry, 2012, 22, 2751-2756.	6.7	135
61	Multifunctional Magnetic Composite Microspheres with in Situ Growth Au Nanoparticles: A Highly Efficient Catalyst System. Journal of Physical Chemistry C, 2011, 115, 1614-1619.	1.5	132
62	Flexible 3D porous CuO nanowire arrays for enzymeless glucose sensing: in situ engineered versus ex situ piled. Nanoscale, 2015, 7, 559-569.	2.8	131
63	Preparation and physicochemical properties of a novel hydroxyapatite/chitosan–silk fibroin composite. Carbohydrate Polymers, 2007, 68, 740-745.	5.1	130
64	Confined Synthesis of FeS ₂ Nanoparticles Encapsulated in Carbon Nanotube Hybrids for Ultrastable Lithium-Ion Batteries. ACS Sustainable Chemistry and Engineering, 2016, 4, 4251-4255.	3.2	126
65	Fabrication and electrochemical characterization of polyaniline nanorods modified with sulfonated carbon nanotubes for supercapacitor applications. Electrochimica Acta, 2011, 56, 1366-1372.	2.6	125
66	Dispersed CuO Nanoparticles on a Silicon Nanowire for Improved Performance of Nonenzymatic H ₂ O ₂ Detection. ACS Applied Materials & Interfaces, 2014, 6, 7055-7062.	4.0	123
67	Moâ€Based Ultrasmall Nanoparticles on Hierarchical Carbon Nanosheets for Superior Lithium Ion Storage and Hydrogen Generation Catalysis. Advanced Energy Materials, 2017, 7, 1602782.	10.2	123
68	Effects of surface modification of fumed silica on interfacial structures and mechanical properties of poly(vinyl chloride) composites. European Polymer Journal, 2006, 42, 1643-1652.	2.6	122
69	Electrocatalytic Oxidation of Glucose by the Glucose Oxidase Immobilized in Grapheneâ€Auâ€Nafion Biocomposite. Electroanalysis, 2010, 22, 259-264.	1.5	122
70	Ultrasound-Triggered Smart Drug Release from Multifunctional Coreâ^'Shell Capsules One-Step Fabricated by Coaxial Electrospray Method. Langmuir, 2011, 27, 1175-1180.	1.6	119
71	Enhanced visible light photocatalytic activity of interlayer-isolated triplex Ag@SiO2@TiO2 core–shell nanoparticles. Nanoscale, 2013, 5, 3359.	2.8	119
72	Phosphorus-driven mesoporous Co3O4 nanosheets with tunable oxygen vacancies for the enhanced oxygen evolution reaction. Electrochimica Acta, 2018, 259, 962-967.	2.6	119

#	Article	IF	CITATIONS
73	Highly conductive and stretchable polymer composites based on graphene/MWCNT network. Chemical Communications, 2013, 49, 1612.	2.2	114
74	Activated nitrogen-doped carbon nanofibers with hierarchical pore as efficient oxygen reduction reaction catalyst for microbial fuel cells. Journal of Power Sources, 2014, 266, 36-42.	4.0	113
75	Tailored graphene-encapsulated mesoporous Co3O4 composite microspheres for high-performance lithium ion batteries. Journal of Materials Chemistry, 2012, 22, 17278.	6.7	112
76	Highly conductive and flexible polymer composites with improved mechanical and electromagnetic interference shielding performances. Nanoscale, 2014, 6, 3796-3803.	2.8	111
77	MnO ₂ nanoflake/polyaniline nanorod hybrid nanostructures on graphene paper for high-performance flexible supercapacitor electrodes. Journal of Materials Chemistry A, 2015, 3, 17165-17171.	5.2	109
78	Rheological Behavior of Titanium Dioxide Suspensions. Journal of Colloid and Interface Science, 2001, 236, 96-103.	5.0	107
79	Controlled Synthesis of Ultrathin Hollow Mesoporous Carbon Nanospheres for Supercapacitor Applications. Industrial & Engineering Chemistry Research, 2014, 53, 3125-3130.	1.8	106
80	Dynamically Formed Surfactant Assembly at the Electrified Electrode–Electrolyte Interface Boosting CO ₂ Electroreduction. Journal of the American Chemical Society, 2022, 144, 6613-6622.	6.6	106
81	Fabrication of Highly Stretchable Conductors Based on 3D Printed Porous Poly(dimethylsiloxane) and Conductive Carbon Nanotubes/Graphene Network. ACS Applied Materials & Interfaces, 2016, 8, 2187-2192.	4.0	104
82	Nanostructured Ternary Nanocomposite of rGO/CNTs/MnO ₂ for High-Rate Supercapacitors. ACS Sustainable Chemistry and Engineering, 2014, 2, 70-74.	3.2	102
83	2D MoS ₂ /polyaniline heterostructures with enlarged interlayer spacing for superior lithium and sodium storage. Journal of Materials Chemistry A, 2017, 5, 5383-5389.	5.2	102
84	Flexible hemispheric microarrays of highly pressure-sensitive sensors based on breath figure method. Nanoscale, 2018, 10, 10691-10698.	2.8	102
85	Interfacial structures and mechanical properties of PVC composites reinforced by CaCO3 with different particle sizes and surface treatments. Polymer International, 2006, 55, 158-164.	1.6	100
86	Electrorheological characteristics of polyaniline/titanate composite nanotube suspensions. Colloid and Polymer Science, 2009, 287, 435-441.	1.0	100
87	BiPO ₄ â€Derived 2D Nanosheets for Efficient Electrocatalytic Reduction of CO ₂ to Liquid Fuel. Angewandte Chemie - International Edition, 2021, 60, 7681-7685.	7.2	98
88	Morphology and properties of ultrafine SnO2–TiO2 coupled semiconductor particles. Materials Chemistry and Physics, 2000, 62, 62-67.	2.0	97
89	CoP nanoparticles anchored on N,P-dual-doped graphene-like carbon as a catalyst for water splitting in non-acidic media. Nanoscale, 2018, 10, 2603-2612.	2.8	96
90	2D nanosheets-based novel architectures: Synthesis, assembly and applications. Nano Today, 2016, 11, 483-520.	6.2	95

#	Article	IF	CITATIONS
91	The pivotal effect of the interaction between reactant and anatase TiO2 nanosheets with exposed {0 0 1} facets on photocatalysis for the photocatalytic purification of VOCs. Applied Catalysis B: Environmental, 2016, 181, 625-634.	10.8	95
92	Controlled synthesis of hierarchical polyaniline nanowires/ordered bimodal mesoporous carbon nanocomposites with high surface area for supercapacitor electrodes. Journal of Power Sources, 2013, 240, 544-550.	4.0	94
93	A Highly Efficient Catalyst toward Oxygen Reduction Reaction in Neutral Media for Microbial Fuel Cells. Industrial & Engineering Chemistry Research, 2013, 52, 6076-6082.	1.8	93
94	Promoting CO2 methanation via ligand-stabilized metal oxide clusters as hydrogen-donating motifs. Nature Communications, 2020, 11, 6190.	5.8	93
95	Multifunctional Fe ₃ O ₄ @Ag/SiO ₂ /Au Core–Shell Microspheres as a Novel SERS-Activity Label via Long-Range Plasmon Coupling. Langmuir, 2013, 29, 690-695.	1.6	92
96	Interfacial charge polarization in Co2P2O7@N, P co-doped carbon nanocages as Mott-Schottky electrocatalysts for accelerating oxygen evolution reaction. Applied Catalysis B: Environmental, 2020, 268, 118417.	10.8	90
97	Synthesis and characterization of polypyrrole/graphite oxide composite by <i>in situ</i> emulsion polymerization. Journal of Polymer Science, Part B: Polymer Physics, 2010, 48, 1329-1335.	2.4	89
98	Synthesis and photocatalysis of hierarchical heteroassemblies of ZnO branched nanorod arrays on Ag core nanowires. Nanoscale, 2012, 4, 5895.	2.8	89
99	Conducting polypyrrole confined in ordered mesoporous silica SBA-15 channels: Preparation and its electrorheology. Microporous and Mesoporous Materials, 2006, 93, 263-269.	2.2	88
100	Planar scattering from hierarchical anatase TiO2 nanoplates with variable shells to improve light harvesting in dye-sensitized solar cells. Chemical Communications, 2011, 47, 5046.	2.2	87
101	Low-temperature processed In2S3 electron transport layer for efficient hybrid perovskite solar cells. Nano Energy, 2017, 36, 102-109.	8.2	87
102	Iron oxide containing graphene/carbon nanotube based carbon aerogel as an efficient E-Fenton cathode for the degradation of methyl blue. Electrochimica Acta, 2016, 200, 75-83.	2.6	86
103	Synergetic effects of nitrogen doping and Au loading on enhancing the visible-light photocatalytic activity of nano-TiO2. Catalysis Communications, 2009, 10, 925-929.	1.6	85
104	A three-dimensional ordered mesoporous carbon/carbon nanotubes nanocomposites for supercapacitors. Journal of Power Sources, 2014, 246, 402-408.	4.0	85
105	Faceâ€ŧoâ€Face Contact and Openâ€Void Coinvolved Si/C Nanohybrids Lithiumâ€Ion Battery Anodes with Extremely Long Cycle Life. Advanced Functional Materials, 2015, 25, 5395-5401.	7.8	85
106	Sprayâ€Assisted Coil–Globule Transition for Scalable Preparation of Waterâ€Resistant CsPbBr ₃ @PMMA Perovskite Nanospheres with Application in Live Cell Imaging. Small, 2018, 14, e1803156.	5.2	85
107	Acetate-derived ZnO ultrafine particles synthesized by spray pyrolysis. Powder Technology, 1998, 100, 20-23.	2.1	83
108	Highly dual-doped multilayer nanoporous graphene: efficient metal-free electrocatalysts for the hydrogen evolution reaction. Journal of Materials Chemistry A, 2015, 3, 12642-12645.	5.2	83

#	Article	IF	CITATIONS
109	Multimetallic Ni–Mo/Cu nanowires as nonprecious and efficient full water splitting catalyst. Journal of Materials Chemistry A, 2017, 5, 4207-4214.	5.2	83
110	Hunting ionic liquids with large electrochemical potential windows. AICHE Journal, 2019, 65, 804-810.	1.8	83
111	Combustion synthesis and photoluminescence of nanocrystals with addition. Journal of Crystal Growth, 2006, 289, 400-404.	0.7	81
112	A Bandâ€Edge Potential Gradient Heterostructure to Enhance Electron Extraction Efficiency of the Electron Transport Layer in Highâ€Performance Perovskite Solar Cells. Advanced Functional Materials, 2017, 27, 1700878.	7.8	81
113	Interface-strengthened CoP nanosheet array with Co2P nanoparticles as efficient electrocatalysts for overall water splitting. Journal of Energy Chemistry, 2019, 37, 1-6.	7.1	81
114	Amperometric glutamate biosensor based on self-assembling glutamate dehydrogenase and dendrimer-encapsulated platinum nanoparticles onto carbon nanotubes. Talanta, 2007, 73, 438-443.	2.9	80
115	Solution-Phase Synthesis of Spherical Zinc Sulfide Nanostructures. Langmuir, 2006, 22, 1329-1332.	1.6	79
116	Upconversion fluorescent strip sensor for rapid determination of Vibrio anguillarum. Nanoscale, 2014, 6, 3804-3809.	2.8	79
117	3D nitrogen-doped graphene foams embedded with ultrafine TiO2 nanoparticles for high-performance lithium-ion batteries. Journal of Materials Chemistry A, 2014, 2, 11124.	5.2	78
118	Graphene/carbon-coated Fe ₃ O ₄ nanoparticle hybrids for enhanced lithium storage. Journal of Materials Chemistry A, 2015, 3, 2361-2369.	5.2	78
119	Continuous oxygen vacancy engineering of the Co ₃ O ₄ layer for an enhanced alkaline electrocatalytic hydrogen evolution reaction. Journal of Materials Chemistry A, 2019, 7, 13506-13510.	5.2	78
120	Fluorine-triggered surface reconstruction of Ni3S2 electrocatalysts towards enhanced water oxidation. Chemical Engineering Journal, 2021, 411, 128488.	6.6	78
121	Biosensor Based on Self-Assembling Glucose Oxidase and Dendrimer-Encapsulated Pt Nanoparticles on Carbon Nanotubes for Glucose Detection. Electroanalysis, 2007, 19, 717-722.	1.5	77
122	Perovskite quantum dots encapsulated in electrospun fiber membranes as multifunctional supersensitive sensors for biomolecules, metal ions and pH. Nanoscale Horizons, 2017, 2, 225-232.	4.1	77
123	Preparation and Application of Mediatorâ€Free H ₂ O ₂ Biosensors of Grapheneâ€Fe ₃ O ₄ Composites. Electroanalysis, 2011, 23, 862-869.	1.5	75
124	Fabrication of polyaniline/mesoporous carbon/MnO2 ternary nanocomposites and their enhanced electrochemical performance for supercapacitors. Electrochimica Acta, 2012, 71, 27-32.	2.6	75
125	Facile synthesis of copper doped carbon dots and their application as a "turn-off―fluorescent probe in the detection of Fe ³⁺ ions. RSC Advances, 2016, 6, 28745-28750.	1.7	75
126	Synthesis and electrorheological characteristics of sea urchin-like TiO2 hollow spheres. Colloid and Polymer Science, 2011, 289, 799-805.	1.0	73

#	Article	lF	CITATIONS
127	Mesoporous single crystals Li ₄ Ti ₅ O ₁₂ grown on rGO as high-rate anode materials for lithium-ion batteries. Chemical Communications, 2014, 50, 8856-8859.	2.2	73
128	MnO2 nanoflakes/hierarchical porous carbon nanocomposites for high-performance supercapacitor electrodes. Electrochimica Acta, 2015, 164, 252-259.	2.6	73
129	Lightâ€Motivated SnO ₂ /TiO ₂ Heterojunctions Enabling the Breakthrough in Energy Density for Lithiumâ€Ion Batteries. Advanced Materials, 2021, 33, e2103558.	11.1	73
130	Formation of polymer/carbon nanotubes nano-hybrid shish–kebab via non-isothermal crystallization. Polymer, 2009, 50, 3835-3840.	1.8	72
131	Tailorable surface sulfur chemistry of mesoporous Ni ₃ S ₂ particles for efficient oxygen evolution. Journal of Materials Chemistry A, 2019, 7, 7548-7552.	5.2	72
132	Shape-controlled synthesis of CeOHCO3 and CeO2 microstructures. Journal of Crystal Growth, 2007, 307, 386-394.	0.7	71
133	Multifunctional Fe ₃ O ₄ @TiO ₂ @Au magnetic microspheres as recyclable substrates for surface-enhanced Raman scattering. Nanoscale, 2014, 6, 5971-5979.	2.8	71
134	Positively charged Pt-based cocatalysts: an orientation for achieving efficient photocatalytic water splitting. Journal of Materials Chemistry A, 2020, 8, 17-26.	5.2	71
135	Large-Scaled, Uniform, Monodispersed ZnO Colloidal Microspheres. Journal of Physical Chemistry C, 2008, 112, 12138-12141.	1.5	70
136	Few-layer MoS2 nanosheets incorporated into hierarchical porous carbon for lithium-ion batteries. Chemical Engineering Journal, 2016, 288, 179-184.	6.6	69
137	Morphology-controllable synthesis of MnO2 hollow nanospheres and their supercapacitive performance. New Journal of Chemistry, 2013, 37, 722.	1.4	68
138	Reciprocal hybridization of MoO ₂ nanoparticles and few-layer MoS ₂ for stable lithium-ion batteries. Chemical Communications, 2015, 51, 13838-13841.	2.2	67
139	In-situ SERS monitoring of reaction catalyzed by multifunctional Fe3O4@TiO2@Ag-Au microspheres. Applied Catalysis B: Environmental, 2017, 205, 11-18.	10.8	67
140	Towards high-performance all-solid-state asymmetric supercapacitors: A hierarchical doughnut-like Ni3S2@PPy coreâ^'shell heterostructure on nickel foam electrode and density functional theory calculations. Journal of Power Sources, 2021, 501, 230003.	4.0	67
141	Functional mesoporous carbon nanotubes and their integration in situ with metal nanocrystals for enhanced electrochemical performances. Chemical Communications, 2011, 47, 8590.	2.2	66
142	Irradiation preparation of reduced graphene oxide/carbon nanotube composites for high-performance supercapacitors. Journal of Power Sources, 2014, 245, 436-444.	4.0	66
143	Ultrathin MnO ₂ nanoflakes grown on N-doped carbon nanoboxes for high-energy asymmetric supercapacitors. Journal of Materials Chemistry A, 2015, 3, 21337-21342.	5.2	66
144	Immobilization of horseradish peroxidase in three-dimensional macroporous TiO2 matrices for biosensor applications. Electrochimica Acta, 2009, 54, 2823-2827.	2.6	65

#	Article	IF	CITATIONS
145	Boosting reaction kinetics and reversibility in Mott-Schottky VS2/MoS2 heterojunctions for enhanced lithium storage. Science Bulletin, 2020, 65, 1470-1478.	4.3	64
146	Metal-enhanced fluorescence of carbon dots adsorbed Ag@SiO2 core-shell nanoparticles. RSC Advances, 2012, 2, 1765.	1.7	63
147	Hollow LiMn ₂ O ₄ Nanocones as Superior Cathode Materials for Lithiumâ€lon Batteries with Enhanced Power and Cycle Performances. Small, 2014, 10, 1096-1100.	5.2	63
148	Kirigami-patterned highly stretchable conductors from flexible carbon nanotube-embedded polymer films. Journal of Materials Chemistry C, 2017, 5, 8714-8722.	2.7	63
149	Integrated Reference Electrodes in Anion-Exchange-Membrane Electrolyzers: Impact of Stainless-Steel Gas-Diffusion Layers and Internal Mechanical Pressure. ACS Energy Letters, 2021, 6, 305-312.	8.8	63
150	Facile flame synthesis and photoluminescent properties of core/shell TiO2/SiO2 nanoparticles. Journal of Alloys and Compounds, 2007, 432, L5-L9.	2.8	62
151	Surfactant-assisted polypyrrole/titanate composite nanofibers: Morphology, structure and electrical properties. Synthetic Metals, 2008, 158, 953-957.	2.1	62
152	In Situ Loading of Cu ₂ O Active Sites on Island-like Copper for Efficient Electrochemical Reduction of Nitrate to Ammonia. ACS Applied Materials & Interfaces, 2022, 14, 6680-6688.	4.0	62
153	Hierarchical porous CoS2 microboxes for efficient oxygen evolution reaction. Electrochimica Acta, 2018, 278, 219-225.	2.6	61
154	Amperometric biosensor based on carbon nanotubes coated with polyaniline/dendrimer-encapsulated Pt nanoparticles for glucose detection. Materials Science and Engineering C, 2009, 29, 1306-1310.	3.8	60
155	Interface-engineered MoS2/C nanosheet heterostructure arrays for ultra-stable sodium-ion batteries. Chemical Engineering Science, 2017, 174, 104-111.	1.9	60
156	Synthesis and structural properties of polypyrrole/nano-Y 2 O 3 conducting composite. Applied Surface Science, 2006, 253, 1736-1740.	3.1	59
157	Hierarchical interconnected macro-/mesoporous Co-containing N-doped carbon for efficient oxygen reduction reactions. Journal of Materials Chemistry A, 2013, 1, 12074.	5.2	59
158	Hierarchical porous iron and nitrogen co-doped carbons as efficient oxygen reduction electrocatalysts in neutral media. Journal of Power Sources, 2014, 265, 246-253.	4.0	59
159	Interfacial Confined Formation of Mesoporous Spherical TiO ₂ Nanostructures with Improved Photoelectric Conversion Efficiency. Inorganic Chemistry, 2010, 49, 5453-5459.	1.9	58
160	Binder-free Co(OH)2 nanoflake–ITO nanowire heterostructured electrodes for electrochemical energy storage with improved high-rate capabilities. Journal of Materials Chemistry, 2011, 21, 10482.	6.7	58
161	Hydrothermal synthesis of hollow Mn2O3 nanocones as anode material for Li-ion batteries. RSC Advances, 2013, 3, 19778.	1.7	58
162	A graphene/carbon nanotube@ï€-conjugated polymer nanocomposite for high-performance organic supercapacitor electrodes. Journal of Materials Chemistry A, 2015, 3, 3880-3890.	5.2	58

#	Article	IF	CITATIONS
163	Electrorheological properties of new mesoporous material with conducting polypyrrole in mesoporous silica. Microporous and Mesoporous Materials, 2006, 94, 193-199.	2.2	57
164	Plasmon-enhanced efficient dye-sensitized solar cells using core–shell-structured β-NaYF ₄ :Yb,Er@SiO ₂ @Au nanocomposites. Journal of Materials Chemistry A, 2014, 2, 16523-16530.	5.2	57
165	Self-Volatilization Approach to Mesoporous Carbon Nanotube/Silver Nanoparticle Hybrids: The Role of Silver in Boosting Li Ion Storage. ACS Nano, 2016, 10, 1648-1654.	7.3	56
166	Synthesis of Anatase TiO ₂ Nanoshuttles by Self-Sacrificing of Titanate Nanowires. Inorganic Chemistry, 2009, 48, 9732-9736.	1.9	55
167	Preparation of polydopamine-functionalized graphene–Fe ₃ O ₄ magnetic composites with high adsorption capacities. RSC Advances, 2014, 4, 30536-30541.	1.7	55
168	A Highly Stretchable, Sensitive, and Transparent Strain Sensor Based on Binary Hybrid Network Consisting of Hierarchical Multiscale Metal Nanowires. Advanced Materials Technologies, 2018, 3, 1800020.	3.0	55
169	Boosting water oxidation electrocatalysts with surface engineered amorphous cobalt hydroxide nanoflakes. Nanoscale, 2018, 10, 12991-12996.	2.8	55
170	Use of a water-in-salt electrolyte to avoid organic material dissolution and enhance the kinetics of aqueous potassium ion batteries. Sustainable Energy and Fuels, 2020, 4, 128-131.	2.5	55
171	Amorphous vanadium oxides with metallic character for asymmetric supercapacitors. Chemical Engineering Journal, 2021, 403, 126380.	6.6	55
172	Synthesis and characterization of new mesoporous material with conducting polypyrrole confined in mesoporous silica. Materials Chemistry and Physics, 2006, 98, 504-508.	2.0	54
173	Crystallinity of Li-doped MgO:Dy3+ nanocrystals via combustion process and their photoluminescence properties. Journal of Alloys and Compounds, 2008, 453, 361-365.	2.8	54
174	Ultrafine V ₂ O ₃ Nanowire Embedded in Carbon Hybrids with Enhanced Lithium Storage Capability. Industrial & Engineering Chemistry Research, 2015, 54, 2960-2965.	1.8	54
175	Influence of Precalcination and Boron-Doping on the Initial Photoluminescent Properties of SrAl ₂ O ₄ :Eu,Dy Phosphors. Crystal Growth and Design, 2008, 8, 3175-3179.	1.4	53
176	Highly stable CsPbBr ₃ @SiO ₂ nanocomposites prepared <i>via</i> confined condensation for use as a luminescent ink. Chemical Communications, 2018, 54, 8064-8067.	2.2	53
177	Local structure tuning in Fe-N-C catalysts through support effect for boosting CO2 electroreduction. Applied Catalysis B: Environmental, 2020, 272, 118960.	10.8	53
178	Sensitive Biosensors Based on (Dendrimer Encapsulated Pt Nanoparticles)/Enzyme Multilayers. Electroanalysis, 2007, 19, 698-703.	1.5	52
179	Self-assembled CNTs/CdS/dehydrogenase hybrid-based amperometric biosensor triggered by photovoltaic effect. Biosensors and Bioelectronics, 2008, 24, 319-323.	5.3	52
180	Dual-defective Co3O4 nanoarrays enrich target intermediates and promise high-efficient overall water splitting. Chemical Engineering Journal, 2021, 424, 130328.	6.6	52

#	Article	IF	CITATIONS
181	Aluminum hydroxide filled ethylene vinyl acetate (EVA) composites: effect of the interfacial compatibilizer and the particle size. Journal of Materials Science, 2007, 42, 4227-4232.	1.7	51
182	Crystallization behavior and UVâ€protection property of PETâ€ZnO nanocomposites prepared by <i>in situ</i> polymerization. Journal of Applied Polymer Science, 2009, 114, 1303-1311.	1.3	51
183	Dual Tuning of Biomass-Derived Hierarchical Carbon Nanostructures for Supercapacitors: the Role of Balanced Meso/Microporosity and Graphene. Scientific Reports, 2015, 5, 15936.	1.6	51
184	Synergistic Enhancement Effect of Al Doping and Highly Active Facets of LiMn ₂ O ₄ Cathode Materials for Lithium-Ion Batteries. Industrial & Engineering Chemistry Research, 2015, 54, 3800-3805.	1.8	51
185	Interface engineering of few-layered MoS2 nanosheets with ultrafine TiO2 nanoparticles for ultrastable Li-ion batteries. Chemical Engineering Journal, 2018, 345, 320-326.	6.6	51
186	A Glucose Biosensor Based on Immobilization of Glucose Oxidase into 3D Macroporous TiO ₂ . Electroanalysis, 2008, 20, 2223-2228.	1.5	50
187	Fabrication of Spherical Multi-Hollow TiO ₂ Nanostructures for Photoanode Film with Enhanced Light-Scattering Performance. Industrial & Engineering Chemistry Research, 2012, 51, 2838-2845.	1.8	50
188	Ultrasensitive and recyclable SERS substrate based on Au-decorated Si nanowire arrays. Dalton Transactions, 2013, 42, 14324.	1.6	50
189	Intrinsic Apyraseâ€Like Activity of Ceriumâ€Based Metal–Organic Frameworks (MOFs): Dephosphorylation of Adenosine Tri―and Diphosphate. Angewandte Chemie - International Edition, 2020, 59, 22952-22956.	7.2	50
190	Tracking structural evolution: <i>operando</i> regenerative CeOx/Bi interface structure for high-performance CO2 electroreduction. National Science Review, 2021, 8, nwaa187.	4.6	50
191	Toughness mechanism in polypropylene composites: Polypropylene toughened with elastomer and calcium carbonate. Journal of Polymer Science, Part B: Polymer Physics, 2004, 42, 1656-1662.	2.4	49
192	Synthesis and characterization of carbon-coated iron core/shell nanostructures. Journal of Alloys and Compounds, 2008, 448, 272-276.	2.8	49
193	Photoluminescence enhancement of carbon dots by gold nanoparticles conjugated via PAMAM dendrimers. Nanoscale, 2013, 5, 11200.	2.8	49
194	Flame synthesis of single crystalline SnO nanoplatelets for lithium-ion batteries. Chemical Engineering Journal, 2014, 242, 220-225.	6.6	49
195	Highly stretchable and transparent triboelectric nanogenerator based on multilayer structured stable electrode for self-powered wearable sensor. Nano Energy, 2020, 78, 105385.	8.2	49
196	General Flame Approach to Chainlike MFe ₂ O ₄ Spinel (M = Cu, Ni, Co, Zn) Nanoaggregates for Reduction of Nitroaromatic Compounds. Industrial & Engineering Chemistry Research, 2015, 54, 9750-9757.	1.8	48
197	Porous CoS nanosheets coated by N and S doped carbon shell on graphene foams for free-standing and flexible lithium ion battery anodes: Influence of void spaces, shell and porous nanosheet. Electrochimica Acta, 2018, 271, 242-251.	2.6	48
198	Bulk Mg-doping and surface polypyrrole-coating enable high-rate and long-life for Ni-rich layered cathodes. Chemical Engineering Journal, 2021, 412, 128625.	6.6	48

#	Article	IF	CITATIONS
199	Synthesis and optical properties of SnO ₂ nanorods. Nanotechnology, 2008, 19, 095708.	1.3	47
200	Gold-coated silica-fiber hybrid materials for application in a novel hydrogen peroxide biosensor. Biosensors and Bioelectronics, 2012, 34, 132-136.	5.3	47
201	Au decorated Fe ₃ O ₄ @TiO ₂ magnetic composites with visible light-assisted enhanced catalytic reduction of 4-nitrophenol. RSC Advances, 2015, 5, 50454-50461.	1.7	47
202	Three-dimensional porous stretchable and conductive polymer composites based on graphene networks grown by chemical vapour deposition and PEDOT:PSS coating. Chemical Communications, 2015, 51, 3169-3172.	2.2	47
203	A flexible freestanding Si/rGO hybrid film anode for stable Li-ion batteries. Journal of Power Sources, 2016, 307, 214-219.	4.0	47
204	Three-dimensionally grown thorn-like Cu nanowire arrays by fully electrochemical nanoengineering for highly enhanced hydrazine oxidation. Nanoscale, 2016, 8, 5810-5814.	2.8	47
205	Magnetic composite microspheres with exposed {001} faceted TiO2 shells: a highly active and selective visible-light photocatalyst. Journal of Materials Chemistry, 2012, 22, 13341.	6.7	46
206	In Situ Deposition of Hierarchical Architecture Assembly from Sn-Filled CNTs for Lithium-Ion Batteries. ACS Applied Materials & Interfaces, 2013, 5, 6672-6677.	4.0	46
207	Mesoporous single-crystalline V ₂ O ₅ nanorods assembled into hollow microspheres as cathode materials for high-rate and long-life lithium-ion batteries. Chemical Communications, 2014, 50, 13362-13365.	2.2	46
208	A silk fibroin based green nano-filter for air filtration. RSC Advances, 2018, 8, 8181-8189.	1.7	46
209	Bridging boron nitride nanosheets with oriented carbon nanotubes by electrospinning for the fabrication of thermal conductivity enhanced flexible nanocomposites. Composites Science and Technology, 2020, 200, 108429.	3.8	46
210	Ultra-fast construction of plaque-like Li2TiO3/TiO2 heterostructure for efficient gas-solid phase CO2 photoreduction. Applied Catalysis B: Environmental, 2020, 269, 118810.	10.8	46
211	An enhanced biosensor for glutamate based on self-assembled carbon nanotubes and dendrimer-encapsulated platinum nanobiocomposites-doped polypyrrole film. Analytica Chimica Acta, 2007, 597, 145-150.	2.6	45
212	Peapod-like nickel@mesoporous carbon core-shell nanowires: a novel electrode material for supercapacitors. RSC Advances, 2011, 1, 954.	1.7	45
213	Tailored anisotropic magnetic conductive film assembled from graphene-encapsulated multifunctional magnetic composite microspheres. Journal of Materials Chemistry, 2012, 22, 545-550.	6.7	45
214	Sculpturing metal foams toward bifunctional 3D copper oxide nanowire arrays for pseudo-capacitance and enzyme-free hydrogen peroxide detection. Journal of Materials Chemistry A, 2015, 3, 8734-8741.	5.2	45
215	Nanospaceâ€confined synthesis of coconutâ€like SnS/C nanospheres for highâ€rate and stable lithiumâ€ion batteries. AICHE Journal, 2018, 64, 1965-1974.	1.8	45
216	Preparation of CsPbBr ₃ @PS composite microspheres with high stability by electrospraying. Journal of Materials Chemistry C, 2018, 6, 7971-7975.	2.7	45

#	Article	IF	CITATIONS
217	High-efficiency Mo doping stabilized LiNi0.9Co0.1O2 cathode materials for rapid charging and long-life Li-ion batteries. Chemical Engineering Science, 2020, 217, 115518.	1.9	45
218	Facile Fabrication of Robust Hydrogen Evolution Electrodes under High Current Densities via Pt@Cu Interactions. Advanced Functional Materials, 2021, 31, 2105579.	7.8	45
219	Designed synthesis of graphene–TiO2–SnO2 ternary nanocomposites as lithium-ion anode materials. New Journal of Chemistry, 2013, 37, 3671.	1.4	44
220	Multifunctional MnO ₂ nanosheet-modified Fe ₃ O ₄ @SiO ₂ /NaYF ₄ :Yb, Er nanocomposites as novel drug carriers. Dalton Transactions, 2014, 43, 451-457.	1.6	44
221	Highly Stretchable, Sensitive, and Transparent Strain Sensors with a Controllable In-Plane Mesh Structure. ACS Applied Materials & Interfaces, 2019, 11, 5316-5324.	4.0	44
222	Highly enhanced degradation of dye with well-dispersed TiO2 nanoparticles under visible irradiation. Journal of Alloys and Compounds, 2007, 440, 281-286.	2.8	43
223	Solutionâ^'Chemical Synthesis of Carbon Nanotube/ZnS Nanoparticle Core/Shell Heterostructures. Inorganic Chemistry, 2007, 46, 5343-5348.	1.9	43
224	Directly grown Si nanowire arrays on Cu foam with a coral-like surface for lithium-ion batteries. Nanoscale, 2014, 6, 14441-14445.	2.8	43
225	Mo-Triggered amorphous Ni ₃ S ₂ nanosheets as efficient and durable electrocatalysts for water splitting. Materials Chemistry Frontiers, 2018, 2, 1462-1466.	3.2	43
226	Revealing the Sudden Alternation in Pt@hâ€BN Nanoreactors for Nearly 100% CO ₂ â€toâ€CH ₄ Photoreduction. Advanced Functional Materials, 2021, 31, 2010780.	7.8	43
227	Photoelectrochemical glucose biosensor incorporating CdS nanoparticles. Particuology, 2009, 7, 347-352.	2.0	42
228	A novel catalyst based on electrospun silver-doped silica fibers with ribbon morphology. Journal of Colloid and Interface Science, 2010, 341, 303-310.	5.0	42
229	MXene interlayer anchored Fe3O4 nanocrystals for ultrafast Li-ion batteries. Chemical Engineering Science, 2020, 212, 115342.	1.9	42
230	Dendrimerâ€encapsulated Pt nanoparticles/polyaniline nanofibers for glucose detection. Journal of Applied Polymer Science, 2008, 109, 1802-1807.	1.3	41
231	Hydrothermal synthesis of novel In2O3 microspheres for gas sensors. Chemical Communications, 2009, , 3618.	2.2	41
232	Scalable Preparation of Ultrathin Silica-Coated Ag Nanoparticles for SERS Application. ACS Applied Materials & Interfaces, 2013, 5, 10643-10649.	4.0	41
233	Photoluminescent carbon–nitrogen quantum dots as efficient electrocatalysts for oxygen reduction. Nanoscale, 2015, 7, 2003-2008.	2.8	41
234	Pyrolysis of conjugated nanoporous polycarbazoles to mesoporous N-doped carbon nanotubes as efficient electrocatalysts for the oxygen reduction reaction. Journal of Materials Chemistry A, 2017, 5, 4507-4512.	5.2	41

#	Article	IF	CITATIONS
235	A flexible bimodal sensor based on an electrospun nanofibrous structure for simultaneous pressure–temperature detection. Nanoscale, 2019, 11, 14242-14249.	2.8	41
236	Confining MoS2 nanocrystals in MOF-derived carbon for high performance lithium and potassium storage. Green Energy and Environment, 2021, 6, 75-82.	4.7	41
237	Toughness mechanism of polypropylene/elastomer/filler composites. Journal of Polymer Science, Part B: Polymer Physics, 2005, 43, 1113-1123.	2.4	40
238	Stable field emission performance from urchin-like ZnO nanostructures. Nanotechnology, 2009, 20, 055706.	1.3	40
239	SnO2 nanorod@TiO2 hybrid material for dye-sensitized solar cells. Journal of Materials Chemistry A, 2014, 2, 8266-8272.	5.2	40
240	Green Preparation of Expandable Graphite and Its Application in Flame-Resistance Polymer Elastomer. Industrial & Engineering Chemistry Research, 2017, 56, 5253-5261.	1.8	40
241	2D Metal Chalcogenides Incorporated into Carbon and their Assembly for Energy Storage Applications. Small, 2018, 14, e1800148.	5.2	40
242	Redox-mediated electrosynthesis of ethylene oxide from CO2 and water. Nature Catalysis, 2022, 5, 185-192.	16.1	40
243	Electrical properties and morphology of highly conductive composites based on polypropylene and hybrid fillers. Journal of Industrial and Engineering Chemistry, 2010, 16, 10-14.	2.9	39
244	Homologous V ₂ O ₃ /C box-in-box and V ₂ O ₅ box for lithium-ion full cells. Journal of Materials Chemistry A, 2016, 4, 12030-12035.	5.2	39
245	Salt-Templating Protocol To Realize Few-Layered Ultrasmall MoS ₂ Nanosheets Inlayed into Carbon Frameworks for Superior Lithium-Ion Batteries. ACS Sustainable Chemistry and Engineering, 2016, 4, 1148-1153.	3.2	39
246	Synthesis and magnetic properties of iron/silica core/shell nanostructures. Journal of Alloys and Compounds, 2008, 457, 560-564.	2.8	38
247	Electrocatalytic activity of Pt doped TiO2 nanotubes catalysts for glucose determination. Journal of Alloys and Compounds, 2010, 500, 247-251.	2.8	38
248	Surface-engineering of layered LiNi 0.815 Co 0.15 Al 0.035 O 2 cathode material for high-energy and stable Li-ion batteries. Journal of Energy Chemistry, 2018, 27, 559-564.	7.1	38
249	Engineering TiO ₂ supported Pt sub-nanoclusters <i>via</i> introducing variable valence Co ion in high-temperature flame for CO oxidation. Nanoscale, 2018, 10, 13384-13392.	2.8	38
250	Photonic crystal pH and metal cation sensors based on poly(vinyl alcohol) hydrogel. New Journal of Chemistry, 2012, 36, 1051.	1.4	37
251	Interfacial Synthesis and Supercapacitive Performance of Hierarchical Sulfonated Carbon Nanotubes/Polyaniline Nanocomposites. Industrial & Engineering Chemistry Research, 2012, 51, 3981-3987.	1.8	37
252	Metallic iron nanoparticles: Flame synthesis, characterization and magnetic properties. Particuology, 2013, 11, 460-467.	2.0	37

#	Article	IF	CITATIONS
253	Highly enhanced thermal conductivity of epoxy composites by constructing dense thermal conductive network with combination of alumina and carbon nanotubes. Composites Part A: Applied Science and Manufacturing, 2019, 125, 105496.	3.8	37
254	Synthesis and optical properties of novel red phosphors YNbTiO6:Eu3+ with highly enhanced brightness by Li+ doping. Solid State Sciences, 2009, 11, 1124-1130.	1.5	36
255	Preparation of Highly Conductive Polypyrrole/Graphite Oxide Composites via in situ Polymerization. Journal of Macromolecular Science - Physics, 2009, 48, 1093-1102.	0.4	36
256	Ethanol-assisted multi-sensitive poly(vinyl alcohol) photonic crystal sensor. Chemical Communications, 2011, 47, 5530-5532.	2.2	36
257	Controllable Nanocarving of Anatase TiO ₂ Single Crystals with Reactive {001} Facets. Chemistry - A European Journal, 2011, 17, 6615-6619.	1.7	36
258	Graphene supported mesoporous single crystal silicon on Cu foam as a stable lithium-ion battery anode. Journal of Materials Chemistry A, 2014, 2, 16360-16364.	5.2	36
259	One-step synthesis of SnO _x nanocrystalline aggregates encapsulated by amorphous TiO ₂ as an anode in Li-ion battery. Journal of Materials Chemistry A, 2015, 3, 9982-9988.	5.2	36
260	Dual-conductive N,S co-doped carbon nanoflowers for high-loading quasi-solid-state supercapacitor. Chemical Engineering Science, 2020, 217, 115496.	1.9	36
261	Synergistic Effect of Platinum Single Atoms and Nanoclusters Boosting Electrocatalytic Hydrogen Evolution. CCS Chemistry, 2021, 3, 2539-2547.	4.6	36
262	Flame Synthesis of Ball-in-Shell Structured TiO2 Nanospheres. Industrial & Engineering Chemistry Research, 2009, 48, 735-739.	1.8	35
263	Stable Core Shell Co ₃ Fe ₇ –CoFe ₂ O ₄ Nanoparticles Synthesized via Flame Spray Pyrolysis Approach. Industrial & Engineering Chemistry Research, 2012, 51, 11157-11162.	1.8	35
264	Self-assembling few-layer MoS ₂ nanosheets on a CNT backbone for high-rate and long-life lithium-ion batteries. RSC Advances, 2014, 4, 40368-40372.	1.7	35
265	Conversion of methanol to propylene over hierarchical HZSM-5: the effect of Al spatial distribution. Chemical Communications, 2018, 54, 6032-6035.	2.2	35
266	Efficient Light Scattering from One-Pot Solvothermally Derived TiO2Nanospindles. Industrial & Engineering Chemistry Research, 2011, 50, 9003-9008.	1.8	34
267	A polymer-coated template-confinement CsPbBr ₃ perovskite quantum dot composite. Nanoscale, 2021, 13, 6586-6591.	2.8	34
268	High-energy and low-cost membrane-free chlorine flow battery. Nature Communications, 2022, 13, 1281.	5.8	34
269	Facile and controllable fabrication of three-dimensionally quasi-ordered macroporous TiO2 for high performance lithium-ion battery applications. New Journal of Chemistry, 2013, 37, 1578.	1.4	33
270	Integrated Ni-P-S nanosheets array as superior electrocatalysts for hydrogen generation. Green Energy and Environment, 2017, 2, 112-118.	4.7	33

#	Article	IF	CITATIONS
271	Atomically dispersed Au catalysts supported on CeO ₂ foam: controllable synthesis and CO oxidation reaction mechanism. Nanoscale, 2017, 9, 16817-16825.	2.8	33
272	Non-Negligible Roles of Pore Size Distribution on Electroosmotic Flow in Nanoporous Materials. ACS Nano, 2019, 13, 8185-8192.	7.3	33
273	<i>110th Anniversary:</i> Concurrently Coating and Doping High-Valence Vanadium in Nickel-Rich Lithiated Oxides for High-Rate and Stable Lithium-Ion Batteries. Industrial & Engineering Chemistry Research, 2019, 58, 4108-4115.	1.8	33
274	Densified MoS2/Ti3C2 films with balanced porosity for ultrahigh volumetric capacity sodium-ion battery. Chemical Engineering Journal, 2021, 413, 127479.	6.6	33
275	Preparation and Formation Mechanism of Alumina Hollow Nanospheres via High-Speed Jet Flame Combustion. Industrial & Engineering Chemistry Research, 2007, 46, 8004-8008.	1.8	32
276	Physically Controlled Cross-Linking in Gelated Crystalline Colloidal Array Photonic Crystals. ACS Applied Materials & Interfaces, 2010, 2, 1499-1504.	4.0	32
277	Mixed Solvents Assisted Flame Spray Pyrolysis Synthesis of TiO ₂ Hierarchically Porous Hollow Spheres for Dye-Sensitized Solar Cells. Industrial & Engineering Chemistry Research, 2013, 52, 11029-11035.	1.8	32
278	Multifunctional gadolinium-labeled silica-coated Fe ₃ O ₄ and CuInS ₂ nanoparticles as a platform for in vivo tri-modality magnetic resonance and fluorescence imaging. Journal of Materials Chemistry B, 2015, 3, 2873-2882.	2.9	32
279	One-step rod coating of high-performance silver nanowire–PEDOT:PSS flexible electrodes with enhanced adhesion after sulfuric acid post-treatment. RSC Advances, 2015, 5, 95280-95286.	1.7	32
280	Aerosol synthesis of Graphene-Fe3O4 hollow hybrid microspheres for heterogeneous Fenton and electro-Fenton reaction. Journal of Environmental Chemical Engineering, 2016, 4, 2469-2476.	3.3	32
281	Nanochannel-confined synthesis of Nb2O5/CNTs nanopeapods for ultrastable lithium storage. Electrochimica Acta, 2019, 295, 829-834.	2.6	32
282	InÂsitu processing and properties of nanostructured hydroxyapatite/alginate composite. Journal of Nanoparticle Research, 2009, 11, 691-699.	0.8	31
283	Nanocrystalline Metal Chalcogenides Obtained Open to Air: Synthesis, Morphology, Mechanism, and Optical Properties. Journal of Physical Chemistry C, 2009, 113, 15492-15496.	1.5	31
284	A Cost-Effective Co-precipitation Method for Synthesizing Indium Tin Oxide Nanoparticles without Chlorine Contamination. Journal of Materials Science and Technology, 2010, 26, 1037-1040.	5.6	31
285	Preparation of hollow alumina nanospheres via surfactant-assisted flame spray pyrolysis. Particuology, 2011, 9, 528-532.	2.0	31
286	In situ synthesis of CNTs/Fe–Ni/TiO2 nanocomposite by fluidized bed chemical vapor deposition and the synergistic effect in photocatalysis. Particuology, 2014, 14, 24-32.	2.0	31
287	Halide Ion Intercalated Electrodeposition Synthesis of Co ₃ O ₄ Nanosheets with Tunable Pores on Graphene Foams as Free-Standing and Flexible Li-Ion Battery Anodes. ACS Applied Energy Materials, 2018, 1, 1239-1251.	2.5	31
288	Synthesis and assembly of three-dimensional MoS2/rGO nanovesicles for high-performance lithium storage. Chemical Engineering Journal, 2018, 350, 1066-1072.	6.6	31

#	Article	IF	CITATIONS
289	Highly Stable, Transparent, and Conductive Electrode of Solution-Processed Silver Nanowire-Mxene for Flexible Alternating-Current Electroluminescent Devices. Industrial & Engineering Chemistry Research, 2019, 58, 21485-21492.	1.8	31
290	Highly transparent and scratch resistant polysiloxane coatings containing silica nanoparticles. Journal of Colloid and Interface Science, 2020, 559, 273-281.	5.0	31
291	Preparation and characterization of photocatalytic carbon dots-sensitized electrospun titania nanostructured fibers. Materials Research Bulletin, 2013, 48, 232-237.	2.7	30
292	Hierarchical porous Li4Mn5O12 nano/micro structure as superior cathode materials for Li-ion batteries. Journal of Power Sources, 2014, 261, 306-310.	4.0	30
293	Quantitative analysis of the PtO structure during photocatalytic water splitting by operando XAFS. Journal of Materials Chemistry A, 2017, 5, 20631-20634.	5.2	30
294	Simple Cadmium Sulfide Compound with Stable 95 % Selectivity for Carbon Dioxide Electroreduction in Aqueous Medium. ChemSusChem, 2018, 11, 1421-1425.	3.6	30
295	Edge-enriched MoS2@C/rGO film as self-standing anodes for high-capacity and long-life lithium-ion batteries. Science China Materials, 2021, 64, 96-104.	3.5	30
296	Synthesis of CdSe nanoparticles into the pores of mesoporous silica microspheres. Acta Materialia, 2008, 56, 1144-1150.	3.8	29
297	Efficient Antifungal and Flame-Retardant Properties of ZnO-TiO2-Layered Double-Nanostructures Coated on Bamboo Substrate. Coatings, 2018, 8, 341.	1.2	29
298	Litchi-peel-like hierarchical hollow copper-ceria microspheres: aerosol-assisted synthesis and high activity and stability for catalytic CO oxidation. Nanoscale, 2018, 10, 22775-22786.	2.8	29
299	Synthesis of monodisperse water-stable surface Pb-rich CsPbCl ₃ nanocrystals for efficient photocatalytic CO ₂ reduction. Nanoscale, 2020, 12, 11842-11846.	2.8	29
300	Heterogeneous MoSe ₂ /Nitrogenâ€Dopedâ€Carbon Nanoarrays: Engineering Atomic Interface for Potassiumâ€ion Storage. Advanced Functional Materials, 2022, 32, 2110223.	7.8	29
301	Morphology and structure of nanosized TiO2 particles synthesized by gas-phase reaction. Materials Chemistry and Physics, 2000, 66, 51-57.	2.0	28
302	Isothermal crystallization kinetics and melting behaviour of PET/ATO nanocomposites prepared by in situ polymerization. European Polymer Journal, 2007, 43, 3177-3186.	2.6	28
303	Structural and electrorheological properties of mesoporous silica modified with triethanolamine. Colloids and Surfaces A: Physicochemical and Engineering Aspects, 2008, 318, 169-174.	2.3	28
304	Effect of additives on the structure characteristics, thermal stability, reducibility and catalytic activity of CeO2–ZrO2 solid solution for methane combustion. Journal of Materials Science, 2009, 44, 1294-1301.	1.7	28
305	Facile flame synthesis and electrochemical properties of carbon nanocoils. Journal of Alloys and Compounds, 2009, 473, 351-355.	2.8	28
306	Highly Efficient Dye-Sensitized Solar Cells by Using a Mesostructured Anatase TiO2Electrode with High Dye Loading Capacity. Industrial & Engineering Chemistry Research, 2010, 49, 9111-9116.	1.8	28

#	Article	IF	CITATIONS
307	Dendrimer-encapsulated Pt nanoparticles on mesoporous silica for glucose detection. Journal of Solid State Electrochemistry, 2011, 15, 511-517.	1.2	28
308	Demonstration of Photoluminescence and Metalâ€Enhanced Fluorescence of Exfoliated MoS ₂ . ChemPhysChem, 2012, 13, 699-702.	1.0	28
309	Double-faced Î ³ -Fe2O3 SiO2 nanohybrids: flame synthesis, in situ selective modification and highly interfacial activity. Nanoscale, 2013, 5, 5360.	2.8	28
310	Threeâ€Ðimensional Graphitized Carbon Nanovesicles for Highâ€₽erformance Supercapacitors Based on Ionic Liquids. ChemSusChem, 2014, 7, 777-784.	3.6	28
311	Three-Dimensional Highly Stretchable Conductors from Elastic Fiber Mat with Conductive Polymer Coating. ACS Applied Materials & Interfaces, 2017, 9, 30772-30778.	4.0	28
312	L1 ₂ Atomic Ordered Substrate Enhanced Pt-Skin Cu ₃ Pt Catalyst for Efficient Oxygen Reduction Reaction. ACS Applied Materials & Interfaces, 2018, 10, 38015-38023.	4.0	28
313	Rapid low-temperature synthesis of hollow CuS0.55 nanoparticles for efficient electrocatalytic water oxidation. Chemical Engineering Science, 2019, 195, 665-670.	1.9	28
314	Defect-domains enabling VO2 nanosheet arrays with fast charge transfer for 3.0 V aqueous supercapacitors. Chemical Engineering Journal, 2021, 423, 130208.	6.6	28
315	Mechanical properties of PVC/nano-CaCO3 composites. Journal of Materials Science, 2005, 40, 2097-2098.	1.7	27
316	Facile fabrication and characterization of novel polyaniline/titanate composite nanotubes directed by block copolymer. European Polymer Journal, 2007, 43, 3780-3786.	2.6	27
317	Heteroepitaxial growth of ZnO branches selectively on TiO2 nanorod tips with improved light harvesting performance. Chemical Communications, 2011, 47, 8400.	2.2	27
318	Solvent-assisted poly(vinyl alcohol) gelated crystalline colloidal array photonic crystals. Soft Matter, 2011, 7, 915-921.	1.2	27
319	Effects of macropore size on structural and electrochemical properties of hierarchical porous carbons. Journal of Materials Science, 2012, 47, 6444-6450.	1.7	27
320	Phase-segregation induced growth of core–shell α-Fe2O3/SnO2 heterostructures for lithium-ion battery. CrystEngComm, 2013, 15, 6715.	1.3	27
321	Multifunctional gadolinium-labeled silica-coated core/shell quantum dots for magnetic resonance and fluorescence imaging of cancer cells. RSC Advances, 2014, 4, 20641-20648.	1.7	27
322	Ternary SnO2@PANI/rGO nanohybrids as excellent anode materials for lithium-ion batteries. Electrochimica Acta, 2015, 157, 205-210.	2.6	27
323	Flexible textile electrode with high areal capacity from hierarchical V2O5 nanosheet arrays. Journal of Power Sources, 2017, 357, 71-76.	4.0	27
324	Synthesis of CsPbBr ₃ perovskite nanocrystals with the sole ligand of protonated (3-aminopropyl)triethoxysilane. Journal of Materials Chemistry C, 2019, 7, 7201-7206.	2.7	27

#	Article	IF	CITATIONS
325	In-situ synthesized surface N-doped Pt/TiO2 via flame spray pyrolysis with enhanced thermal stability for CO catalytic oxidation. Applied Surface Science, 2019, 481, 360-368.	3.1	27
326	In situ synthesis of sulfide-coated polystyrene composites for the fabrication of photonic crystals. Journal of Colloid and Interface Science, 2006, 301, 130-136.	5.0	26
327	Fabrication and characterization of mesoporous TiO2/polypyrrole-based nanocomposite for electrorheological fluid. Materials Research Bulletin, 2008, 43, 3263-3269.	2.7	26
328	Flame Synthesis of Tin Oxide Nanorods: A Continuous and Scalable Approach. Journal of Physical Chemistry C, 2010, 114, 5867-5870.	1.5	26
329	Continuous flame synthesis of near surface nitrogen doped TiO2 for dye-sensitized solar cells. Chemical Engineering Journal, 2014, 258, 163-170.	6.6	26
330	Nitrogen-doped Fe ₃ C@C particles as an efficient heterogeneous photo-assisted Fenton catalyst. RSC Advances, 2017, 7, 15168-15175.	1.7	26
331	Tuning Optical Properties of Lead-Free 2D Tin-Based Perovskites with Carbon Chain Spacers. Journal of Physical Chemistry C, 2019, 123, 31279-31285.	1.5	26
332	Impacts on carbon dioxide electroreduction of cadmium sulfides <i>via</i> continuous surface sulfur vacancy engineering. Chemical Communications, 2020, 56, 563-566.	2.2	26
333	Cobalt-stabilized oxygen vacancy of V2O5 nanosheet arrays with delocalized valence electron for alkaline water splitting. Chemical Engineering Science, 2020, 227, 115915.	1.9	26
334	Multivalence-Ion Intercalation Enables Ultrahigh 1T Phase MoS ₂ Nanoflowers to Enhanced Sodium-Storage Performance. CCS Chemistry, 2021, 3, 1472-1482.	4.6	26
335	Isolated ultrasmall Bi nanosheets for efficient CO2-to-formate electroreduction. Nano Research, 2022, 15, 1409-1414.	5.8	26
336	Preparation and properties of poly(ethylene terephthalate)/ATO nanocomposites. Journal of Applied Polymer Science, 2007, 105, 2783-2790.	1.3	25
337	Flame synthesis of carbon nanotubes with high density on stainless steel mesh. Journal of Alloys and Compounds, 2008, 463, 317-322.	2.8	25
338	CoO nanosheets derived from electrodeposited cobalt metal towards high performance lithium ion batteries. Electrochimica Acta, 2016, 222, 1300-1307.	2.6	25
339	Electron transfer effect from Au to Pt in Au-Pt/TiO2 towards efficient catalytic activity in CO oxidation at low temperature. Applied Surface Science, 2020, 521, 146447.	3.1	25
340	Multiwalled Carbon Nanotubes Incorporated with Dendrimer Encapsulated with Pt Nanoparticles: An Attractive Material for Sensitive Biosensors. Chemistry Letters, 2006, 35, 326-327.	0.7	24
341	Thermal conductivity and tribological properties of POM u composites. Polymer Engineering and Science, 2010, 50, 2153-2159.	1.5	24
342	Effect of Surface Structure of Nano-CaCO ₃ Particles on Mechanical and Rheological Properties of PVC Composites. Journal of Macromolecular Science - Physics, 2010, 49, 970-982.	0.4	24

#	Article	IF	CITATIONS
343	Rapid flame synthesis of internal Mo ⁶⁺ doped TiO ₂ nanocrystals in situ decorated with highly dispersed MoO ₃ clusters for lithium ion storage. Nanoscale, 2015, 7, 18603-18611.	2.8	24
344	Polyamide 6 composite with highly improved mechanical properties by PEI-CNT grafted glass fibers through interface wetting, infiltration and crystallization. Polymer, 2019, 172, 253-264.	1.8	24
345	Effective Singlet Oxygen Generation in Silicaâ€Coated CsPbBr ₃ Quantum Dots through Energy Transfer for Photocatalysis. ChemSusChem, 2020, 13, 682-687.	3.6	24
346	Redirecting dynamic structural evolution of nickel-contained RuO2 catalyst during electrochemical oxygen evolution reaction. Journal of Energy Chemistry, 2022, 69, 330-337.	7.1	24
347	Self-assembly of solid or tubular ZnO rods into twinning microprisms via a hydrothermal route. Journal of Alloys and Compounds, 2009, 478, 550-553.	2.8	23
348	Gold/mesoporous silica-fiber core-shell hybrid nanostructure: a potential electron transfer mediator in a bio-electrochemical system. New Journal of Chemistry, 2010, 34, 2166.	1.4	23
349	Facile synthesis of upconversion luminescent mesoporous Y2O3:Er microspheres and metal enhancement using gold nanoparticles. RSC Advances, 2012, 2, 10592.	1.7	23
350	Solar-assisted dual chamber microbial fuel cell with a CuInS ₂ photocathode. RSC Advances, 2014, 4, 23790-23796.	1.7	23
351	Layered Confinement Reaction: Atomicâ€level Dispersed Iron–Nitrogen Coâ€Doped Ultrathin Carbon Nanosheets for CO ₂ Electroreduction. ChemSusChem, 2019, 12, 2644-2650.	3.6	23
352	Internal-diffusion controlled synthesis of V2O5 hollow microspheres for superior lithium-ion full batteries. Chemical Engineering Science, 2019, 200, 38-45.	1.9	23
353	Stretch induced photoluminescence enhanced perovskite quantum dot polymer composites. Journal of Materials Chemistry C, 2020, 8, 1413-1420.	2.7	23
354	Electrorheological behavior of urea-doped mesoporous TiO2 suspensions. Colloids and Surfaces A: Physicochemical and Engineering Aspects, 2006, 280, 71-75.	2.3	22
355	Amperometric glucose biosensor based on platinum nanoparticle encapsulated with a clay. Mikrochimica Acta, 2010, 171, 233-239.	2.5	22
356	Mn-doped 2D Sn-based perovskites with energy transfer from self-trapped excitons to dopants for warm white light-emitting diodes. Journal of Materials Chemistry C, 2020, 8, 8502-8506.	2.7	22
357	Highly dispersed secondary building unit-stabilized binary metal center on a hierarchical porous carbon matrix for enhanced oxygen evolution reaction. Nanoscale, 2021, 13, 1213-1219.	2.8	22
358	Tailoring charge transfer in perovskite quantum dots/black phosphorus nanosheets photocatalyst via aromatic molecules. Applied Surface Science, 2021, 545, 149012.	3.1	22
359	Electrochemical synthesis of magnetic nanoparticles within mesoporous silica microspheres. Colloids and Surfaces A: Physicochemical and Engineering Aspects, 2007, 294, 287-291.	2.3	21
360	ENFET glucose biosensor produced with dendrimer encapsulated Pt nanoparticles. Materials Science and Engineering C, 2008, 28, 1236-1241.	3.8	21

#	Article	IF	CITATIONS
361	Layer-by-Layer Assembly of Aqueous Dispersible, Highly Conductive Poly(aniline-co-o-anisidine)/Poly(sodium 4-styrenesulfonate)/MWNTs Core–Shell Nanocomposites. Langmuir, 2008, 24, 5825-5831.	1.6	21
362	Nanomaterials synthesized by gas combustion flames: Morphology and structure. Particuology, 2010, 8, 556-562.	2.0	21
363	Carbon nanotubes coated with platinum nanoparticles as anode of biofuel cell. Particuology, 2012, 10, 450-455.	2.0	21
364	Construction of core–shell Fe2O3@SnO2 nanohybrids for gas sensors by a simple flame-assisted spray process. RSC Advances, 2013, 3, 22373.	1.7	21
365	Photoelectrochemical Detection of H ₂ O ₂ Based on Flowerâ€Like CuInS ₂ â€Graphene Hybrid. Electroanalysis, 2014, 26, 573-580.	1.5	21
366	Engineering the outermost layers of TiO ₂ nanoparticles using <i>in situ</i> Mg doping in a flame aerosol reactor. AICHE Journal, 2017, 63, 870-880.	1.8	21
367	Macroporous MoS2/carbon hybrid film with superior ion/electron conductivity for superhigh areal capacity Li-ion batteries. Chemical Engineering Science, 2019, 207, 611-618.	1.9	21
368	Multifunctional films with a highly oriented "nano-brick wall―structure by regulating modified TiO ₂ @graphene oxide/poly(vinyl alcohol) nanocomposites. Nanoscale, 2019, 11, 7424-7432.	2.8	21
369	Modified cellulose nanocrystals based on <scp>Slâ€ATRP</scp> for enhancing interfacial compatibility and mechanical performance of biodegradable <scp>PLA</scp> / <scp>PBAT</scp> blend. Polymer Composites, 2022, 43, 3753-3764.	2.3	21
370	Morphology and crystal structure of A1-doped TiO2 nanoparticles synthesized by vapor phase oxidation of titanium tetrachloride. Journal of Non-Crystalline Solids, 2006, 352, 4128-4135.	1.5	20
371	Electrorheological behavior of copper phthalocyanine-doped mesoporous TiO2 suspensions. Journal of Colloid and Interface Science, 2006, 294, 499-503.	5.0	20
372	Preparation and electrorheology of new mesoporous polypyrrole/MCM-41 suspensions. Journal of Materials Science, 2006, 41, 5047-5049.	1.7	20
373	High-affinity integration of hydroxyapatite nanoparticles with chemically modified silk fibroin. Journal of Nanoparticle Research, 2007, 9, 919-929.	0.8	20
374	Highly compressible magnetic liquid marbles assembled from hydrophobic magnetic chain-like nanoparticles. RSC Advances, 2014, 4, 3162-3164.	1.7	20
375	In-situ growth of ultrathin MoS2 nanosheets on sponge-like carbon nanospheres for lithium-ion batteries. Science China Materials, 2018, 61, 1049-1056.	3.5	20
376	CsPbBr3 quantum dots photodetectors boosting carrier transport via molecular engineering strategy. Nano Research, 2021, 14, 4038-4045.	5.8	20
377	Promotional effects of Cu O on the activity of Cu/ZnO catalyst toward efficient CO oxidation. Applied Surface Science, 2021, 548, 149241.	3.1	20
378	Optimizing SnO _{2â^'} <i>_x</i> /Fe ₂ O ₃ Heteroâ€Nanocrystals Toward Rapid and Highly Reversible Lithium Storage. Small, 2021, 17, e2103532.	5.2	20

18

#	Article	IF	CITATIONS
379	Properties of Dendrimer-Encapsulated Pt Nanoparticles Doped Polypyrrole Composite Films and Their Electrocatalytic Activity for Glucose Oxidation. Electroanalysis, 2007, 19, 1677-1682.	1.5	19
380	Surface characteristics and microstructure of dispersed TiO2 nanoparticles prepared by diffusion flame combustion. Materials Chemistry and Physics, 2008, 107, 344-349.	2.0	19
381	Mesoporous Silica Spheres as Microreactors for Performing CdS Nanocrystal Synthesis. Crystal Growth and Design, 2008, 8, 4494-4498.	1.4	19
382	Emulsion Polymerization: A New Approach to Prepare Graphite Oxide Coated with Polyaniline. Journal of Macromolecular Science - Physics, 2009, 48, 226-237.	0.4	19
383	Confined growth of CuO, NiO, and Co3O4 nanocrystals in mesoporous silica (MS) spheres. Journal of Alloys and Compounds, 2011, 509, 2970-2975.	2.8	19
384	Microbial fuel cell cathode with dendrimer encapsulated Pt nanoparticles as catalyst. Journal of Power Sources, 2011, 196, 10611-10615.	4.0	19
385	Polyamide 6 composites reinforced with glass fibers modified with electrostatically assembled multiwall carbon nanotubes. Journal of Materials Science, 2012, 47, 5446-5454.	1.7	19
386	In-situ fabrication of CNT/TiO2 interpenetrating network film on nickel substrate by chemical vapour deposition and application in photoassisted water electrolysis. Catalysis Communications, 2012, 21, 27-31.	1.6	19
387	Sn@Ni ₃ Sn ₄ embedded nanocable-like carbon hybrids for stable lithium-ion batteries. Chemical Communications, 2015, 51, 16373-16376.	2.2	19
388	Aerosol construction of multi-shelled LiMn ₂ O ₄ hollow microspheres as a cathode in lithium ion batteries. New Journal of Chemistry, 2016, 40, 1839-1844.	1.4	19
389	A new method combining modification of montmorillonite and crystal regulation to enhance the mechanical properties of polypropylene. Polymer Testing, 2020, 82, 106236.	2.3	19
390	Dynamic determination of Cu ⁺ roles for CO ₂ reduction on electrochemically stable Cu ₂ O-based nanocubes. Journal of Materials Chemistry A, 2022, 10, 8459-8465.	5.2	19
391	Synthesis of Mesoporous Eu ₂ O ₃ Microspindles. Crystal Growth and Design, 2007, 7, 2670-2674.	1.4	18
392	Mesoporous Carbon Incorporated Metal Oxide Nanomaterials as Supercapacitor Electrodes (Adv.) Tj ETQq0 0 0 r	gBT /Overl 11:1	ock 10 Tf 50
393	Improved photoelectric conversion efficiency from titanium oxide-coupled tin oxide nanoparticles formed in flame. Journal of Power Sources, 2014, 268, 922-927.	4.0	18
394	A novel strategy for the aqueous synthesis of down-/up-conversion nanocomposites for dual-modal cell imaging and drug delivery. Journal of Materials Chemistry B, 2014, 2, 8372-8377.	2.9	18
395	Performance optimization in dye-sensitized solar cells with β-NaYF4:Yb3+,Er3+@SiO2@TiO2 mesoporous microspheres as multi-functional photoanodes. Electrochimica Acta, 2016, 211, 92-100.	2.6	18

³⁹⁶ Locally-ordered PtNiPb ternary nano-pompons as efficient bifunctional oxygen reduction and 2.8 methanol oxidation catalysts. Nanoscale, 2019, 11, 16945-16953.

#	Article	IF	CITATIONS
397	Confining ultrahigh oxygen vacancy SnO2 nanocrystals into nitrogen-doped carbon for enhanced Li-ion storage kinetics and reversibility. Journal of Energy Chemistry, 2022, 69, 450-455.	7.1	18
398	Low full-cell voltage driven high-current-density selective paired formate electrosynthesis. Journal of Materials Chemistry A, 2022, 10, 1329-1335.	5.2	18
399	Copper doped CoSx@Co(OH)2 hierarchical mesoporous nanosheet arrays as binder-free electrodes for superior supercapacitors. Journal of Alloys and Compounds, 2022, 911, 165115.	2.8	18
400	Tunable selectivity on copper–bismuth bimetallic aerogels for electrochemical CO2 reduction. Applied Catalysis B: Environmental, 2022, 317, 121650.	10.8	18
401	Production and characterization of nanocrystalline SnO2 films on Al2O3 agglomerates by CVD in a fluidized bed. Materials Chemistry and Physics, 1999, 59, 130-135.	2.0	17
402	One-pot synthesis of polyaniline-doped in mesoporous TiO2 and its electrorheological behavior. Materials Science and Engineering B: Solid-State Materials for Advanced Technology, 2007, 137, 213-216.	1.7	17
403	Poly(aniline-2-sulfonic acid) modified multiwalled carbon nanotubes with good aqueous dispersibility. Journal of Colloid and Interface Science, 2008, 317, 199-205.	5.0	17
404	Synthesis and electrorheological characteristics of titanate nanotube suspensions under oscillatory shear. Journal of Industrial and Engineering Chemistry, 2009, 15, 550-554.	2.9	17
405	Fabrication of TiO2/CdS composite fiber via an electrospinning method. New Journal of Chemistry, 2010, 34, 1116.	1.4	17
406	A sol–gel method to synthesize indium tin oxide nanoparticles. Particuology, 2011, 9, 471-474.	2.0	17
407	Kinetics of coupling cracking of butene and pentene on modified HZSM-5 catalyst. Chemical Engineering Journal, 2018, 346, 397-405.	6.6	17
408	The Effect of the Coordination Environment of Atomically Dispersed Fe and N Coâ€doped Carbon Nanosheets on CO 2 Electroreduction. ChemElectroChem, 2020, 7, 4767-4772.	1.7	17
409	Strongly coupled N-doped graphene quantum dots/Ni(Fe)OxHy electrocatalysts with accelerated reaction kinetics for water oxidation. Chemical Engineering Journal, 2022, 430, 133068.	6.6	17
410	Enhancing electrocatalytic <scp>N₂</scp> reduction via tailoring the electric double layers. AICHE Journal, 2022, 68, .	1.8	17
411	Self-organized NiO architectures: Synthesis and catalytic properties for growth of carbon nanotubes. Journal of Alloys and Compounds, 2009, 474, 358-363.	2.8	16
412	Template-free synthesis of hollow poly(<i>o</i> -anisidine) microspheres and their electrorheological characteristics. Smart Materials and Structures, 2011, 20, 065014.	1.8	16
413	In situ Au-catalyzed fabrication of branch-type SnO2 nanowires by a continuous gas-phase route for dye-sensitized solar cells. Journal of Materials Chemistry A, 2013, 1, 13814.	5.2	16
414	Water-soluble inorganic photocatalyst for overall water splitting. Applied Catalysis B: Environmental, 2017, 209, 247-252.	10.8	16

#	Article	IF	CITATIONS
415	Sharpâ€Tipped Zinc Nanowires as an Efficient Electrocatalyst for Carbon Dioxide Reduction. Chemistry - A European Journal, 2018, 24, 15486-15490.	1.7	16
416	Exposed Surface Engineering of High-voltage LiNi _{0.5} Co _{0.2} Mn _{0.3} O ₂ Cathode Materials Enables High-rate and Durable Li-ion Batteries. Industrial & Engineering Chemistry Research, 2019, 58, 23099-23105.	1.8	16
417	Ag@Au Core‧hell Nanowires for Nearly 100 % CO ₂ â€ŧo O Electroreduction. Chemistry - a Asian Journal, 2020, 15, 425-431.	ⁱⁿ 1.7	16
418	Pomegranate-like Ti-doped LiNi0.4Mn1.6O4 5ÂV-class cathode with superior high-voltage cycle and rate performance for Li-ion batteries. Chemical Engineering Science, 2021, 231, 116297.	1.9	16
419	Preparation of nanocrystalline SnO2 thin film coated Al2O3 ultrafine particles by fluidized chemical vapor deposition. Thin Solid Films, 1997, 310, 238-243.	0.8	15
420	Inverse Opal of Polyaniline for Biosensors Prepared by Electrochemical and Self-Assembly Techniques. Journal of the Electrochemical Society, 2008, 155, J23.	1.3	15
421	Preparation of azithromycin microcapsules by a layer-by-layer self-assembly approach and release behaviors of azithromycin. Colloids and Surfaces A: Physicochemical and Engineering Aspects, 2010, 362, 135-139.	2.3	15
422	Self-Cleaning Films with High Transparency Based on TiO ₂ Nanoparticles Synthesized via Flame Combustion. Industrial & Engineering Chemistry Research, 2010, 49, 3654-3662.	1.8	15
423	Large-scale, uniform, single-crystalline Cd(OH)2 hexagonal platelets for Cd-based functional applications. CrystEngComm, 2010, 12, 1726.	1.3	15
424	The Effects of Copper and Polytetrafluoroethylene (PTFE) on Thermal Conductivity and Tribological Behavior of Polyoxymethylene (POM) Composites. Journal of Macromolecular Science - Physics, 2011, 50, 2023-2033.	0.4	15
425	A feasible hydrogen evolution process of water electrolysis assisted by TiO2 nanotube photocatalysis. Journal of Industrial and Engineering Chemistry, 2013, 19, 1112-1116.	2.9	15
426	Zinc oxide with dominant (1 0 0) facets boosts vulcanization activity. European Polymer Journal, 2019, 113, 148-154.	2.6	15
427	The combined effect of impregnated rollers configuration and glass fibers surface modification on the properties of continuous glass fibers reinforced polypropylene prepreg composites. Composites Science and Technology, 2020, 197, 108259.	3.8	15
428	Efficient electrocatalytic formic acid oxidation over PdAu-manganese oxide/carbon. Journal of Colloid and Interface Science, 2021, 593, 244-250.	5.0	15
429	Bismuthene with stable Bi O bonds for efficient CO2 electroreduction to formate. Chemical Engineering Science, 2022, 251, 117409.	1.9	15
430	Toward Highâ€Performance CO ₂ â€toâ€C ₂ Electroreduction via Linker Tuning on MOFâ€Derived Catalysts. Small, 2022, 18, e2200720.	5.2	15
431	Significant Improvement in the Flame Retardancy and Thermal Conductivity of the Epoxy Resin via Constructing a Branched Flame Retardant Based on SI-ATRP Initiated by Dopamine-Modified Boron Nitride. Industrial & Engineering Chemistry Research, 2022, 61, 8031-8042.	1.8	15
432	Preparation of phase homogeneous Mn–Zn ferrite powder by spray pyrolysis. Journal of Materials Research, 1999, 14, 3073-3082.	1.2	14

#	Article	IF	CITATIONS
433	The anti-static poly(ethylene terephthalate) nanocomposite fiber byin situ polymerization: The thermo-mechanical and electrical properties. Journal of Applied Polymer Science, 2007, 105, 1490-1495.	1.3	14
434	Nonisothermal crystallization and melting behavior of a luminescent conjugated polymer, poly(9,9-dihexylfluorene-alt-co-2,5-didecyloxy-1,4-phenylene). Journal of Polymer Science, Part B: Polymer Physics, 2007, 45, 976-987.	2.4	14
435	Fabrication and electrochemical property of Ag-doped SiO2 nanostructured ribbons. Colloids and Surfaces A: Physicochemical and Engineering Aspects, 2010, 356, 120-125.	2.3	14
436	Fabrication of TiO2 film with different morphologies on Ni anode and application in photoassisted water electrolysis. Applied Surface Science, 2013, 266, 126-131.	3.1	14
437	Controlled synthesis of mesoporous carbon nanosheets and their enhanced supercapacitive performance. Journal of Solid State Electrochemistry, 2013, 17, 1677-1684.	1.2	14
438	Enhanced Fluorescence of Graphene Oxide by Well-Controlled Au@SiO2 Core-Shell Nanoparticles. Journal of Fluorescence, 2014, 24, 137-141.	1.3	14
439	Macro-mesoporous TiO ₂ Microspheres for Highly Efficient Dye-Sensitized Solar Cells. Industrial & Engineering Chemistry Research, 2015, 54, 6692-6697.	1.8	14
440	Selenium vacancy triggered atomic disordering of Co _{0.85} Se nanoparticles towards a highly-active electrocatalyst for water oxidation. Chemical Communications, 2020, 56, 14451-14454.	2.2	14
441	Highly efficient Au/Fe2O3 for CO oxidation: The vital role of spongy Fe2O3 toward high catalytic activity and stability. Journal of Colloid and Interface Science, 2022, 608, 2181-2191.	5.0	14
442	Introducing the Solvent Coâ€Intercalation Mechanism for Hard Carbon with Ultrafast Sodium Storage. Small, 2022, 18, e2108092.	5.2	14
443	Fe-doped and sulfur-enriched Ni3S2 nanowires with enhanced reaction kinetics for boosting water oxidation. Green Chemical Engineering, 2022, 3, 367-373.	3.3	14
444	Controllable synthesis of carbon nanotubes with ultrafine inner diameters in ethanol flame. Physica B: Condensed Matter, 2007, 398, 18-22.	1.3	13
445	Novel silicaâ€coated iron–carbon composite particles and their targeting effect as a drug carrier. Journal of Biomedical Materials Research - Part A, 2008, 86A, 671-677.	2.1	13
446	Hydrothermal synthesis of ordered nanolamella-composed Y2O3:Eu3+ architectures and their luminescent properties. Physica E: Low-Dimensional Systems and Nanostructures, 2008, 41, 304-308.	1.3	13
447	Synthesis and sintering of indium tin oxide nanoparticles by citrate-nitrate combustion method. Rare Metals, 2010, 29, 355-360.	3.6	13
448	Hydrothermal fabrication of Ni3S2/TiO2 nanotube composite films on Ni anode and application in photoassisted water electrolysis. Journal of Alloys and Compounds, 2013, 574, 217-220.	2.8	13
449	In situ Surface Functionalization of Hydrophilic Silica Nanoparticles via Flame Spray Process. Journal of Materials Science and Technology, 2015, 31, 901-906.	5.6	13
450	Modulating the Volmer Step by MOF Derivatives Assembled with Heterogeneous Ni ₂ P-CoP Nanocrystals in Alkaline Hydrogen Evolution Reaction. Journal of the Electrochemical Society, 2018, 165, F1286-F1291.	1.3	13

#	Article	IF	CITATIONS
451	Construction of Nanoreactors Combining Two-Dimensional Hexagonal Boron Nitride (h-BN) Coating with Pt/Al ₂ O ₃ Catalyst toward Efficient Catalysis for CO Oxidation. Industrial & Engineering Chemistry Research, 2018, 57, 13353-13361.	1.8	13
452	Subnano‣ized Pt–Au Alloyed Clusters as Enhanced Cocatalyst for Photocatalytic Hydrogen Evolution. Chemistry - an Asian Journal, 2019, 14, 2112-2115.	1.7	13
453	Nanospaceâ€Confinement Synthesis: Designing Highâ€Energy Anode Materials toward Ultrastable Lithiumâ€lon Batteries. Small, 2020, 16, e2002351.	5.2	13
454	Fabrication and characterization of cerium-doped titania inverse opal by sol–gel method. Materials Chemistry and Physics, 2007, 106, 209-214.	2.0	12
455	Synthesis of ZnS nanoparticles into the pore of mesoporous silica spheres. Materials Letters, 2009, 63, 1068-1070.	1.3	12
456	A novel approach to prepare PBT nanocomposites with elastomerâ€modified SiO ₂ particles. Polymer Composites, 2009, 30, 673-679.	2.3	12
457	Photoelectronic properties of horseradish peroxidase-functionalized CdSe/silica mesoporous composite and its sensing towards hydrogen peroxide. Journal of Solid State Electrochemistry, 2011, 15, 731-736.	1.2	12
458	Improving photoelectrochemical activity of dye sensitized solar cell by a bilayered electrode with an overlayer of mesoporous anatase TiO2. Particuology, 2011, 9, 222-227.	2.0	12
459	Functional mesoporous carbon-coated CNT network for high-performance supercapacitors. New Journal of Chemistry, 2013, 37, 1294.	1.4	12
460	Effect of phenolic resin infiltration content on the structural and electrochemical properties of hierarchical porous carbons. Journal of Materials Science, 2014, 49, 7489-7496.	1.7	12
461	Comparative Study on Optical Properties and Scratch Resistance of Nanocomposite Coatings Incorporated with Flame Spray Pyrolyzed Silica Modified via in-situ Route and ex-situ Route. Journal of Materials Science and Technology, 2016, 32, 251-258.	5.6	12
462	Porous Pt ₃ Ni with enhanced activity and durability towards oxygen reduction reaction. RSC Advances, 2018, 8, 15344-15351.	1.7	12
463	Rich Bismuthâ€Oxygen Bonds in Bismuth Derivatives from Bi ₂ S ₃ Preâ€Catalysts Promote the Electrochemical Reduction of CO ₂ . ChemElectroChem, 2020, 7, 2864-2868.	1.7	12
464	An ultrasonic atomization spray strategy for constructing hydrophobic and hydrophilic synergistic surfaces as gas diffusion layers for proton exchange membrane fuel cells. Journal of Power Sources, 2020, 451, 227784.	4.0	12
465	Confining ultrafine SnS2 nanoparticles into MXene interlayer toward fast and stable lithium storage. Chemical Engineering Science, 2022, 247, 117087.	1.9	12
466	Stable Bismuthâ€Doped Lead Halide Perovskite Coreâ€Shell Nanocrystals by Surface Segregation Effect. Small, 2022, 18, e2104399.	5.2	12
467	Controllable oxygen vacancy SnO2-x anodes for lithium-ion batteries with high stability. Chemical Engineering Journal, 2022, 437, 135422.	6.6	12
468	Stabilizing surface chemistry and texture of single-crystal Ni-rich cathodes for Li-ion batteries. Journal of Materials Science and Technology, 2022, 125, 192-197.	5.6	12

#	Article	IF	CITATIONS
469	Identifying Activity Trends for the Electrochemical Production of H ₂ O ₂ on M–N–C Single-Atom Catalysts Using Theoretical Kinetic Computations. Journal of Physical Chemistry C, 2022, 126, 10388-10398.	1.5	12
470	Nonisothermal crystallization kinetics of poly(ethylene terephthalate)/antimonyâ€doped tin oxide nanocomposites. Journal of Applied Polymer Science, 2008, 109, 3753-3762.	1.3	11
471	Preparation of silica-sustained electrospun polyvinylpyrrolidone fibers with uniform mesopores via oxidative removal of template molecules by H2O2 treatment. Materials Research Bulletin, 2010, 45, 830-837.	2.7	11
472	Synthesis and Structural and Electrical Characteristics of Polypyrrole Nanotube/TiO2 Hybrid Composites. Journal of Macromolecular Science - Physics, 2010, 49, 419-428.	0.4	11
473	Preparation of monodispersed mesoporous silica spheres with tunable pore size and pore-size effects on adsorption of Au nanoparticles and urease. Materials Science and Engineering C, 2011, 31, 166-172.	3.8	11
474	Direct Growth of Aligned Carbon Nanotubes on Quartz Fibers for Structural Epoxy Composites. Industrial & Engineering Chemistry Research, 2012, 51, 4927-4933.	1.8	11
475	Synthesis of glass fiberâ€multiwall carbon nanotube hybrid structures for highâ€performance conductive composites. Polymer Composites, 2013, 34, 1313-1320.	2.3	11
476	Transcrystalline induced by MWCNTs and organic nucleating agents at the interface of glass fiber/polypropylene. Polymer Composites, 2018, 39, 3424-3433.	2.3	11
477	Preparation of Co–N carbon nanosheet oxygen electrode catalyst by controlled crystallization of cobalt salt precursors for all-solid-state Al–air battery. RSC Advances, 2018, 8, 22193-22198.	1.7	11
478	Facile synthesis of multi-shelled hollow Cu CeO2 microspheres with promoted catalytic performance for preferential oxidation of CO. Materials Chemistry and Physics, 2019, 226, 158-168.	2.0	11
479	Hierarchical TiO2 microspheres with enlarged lattice spacing for rapid and ultrastable sodium storage. Chemical Engineering Science, 2021, 231, 116298.	1.9	11
480	Efficient CO ₂ Electroreduction on Ag ₂ S Nanodots Modified CdS Nanorods as Cooperative Catalysts. ChemCatChem, 2021, 13, 1161-1164.	1.8	11
481	Derived CuSn Alloys from Heterointerfaces in Bimetallic Oxides Promote the CO ₂ Electroreduction to Formate. ChemElectroChem, 2021, 8, 1150-1155.	1.7	11
482	Fluorine-activation driving surface reconstruction on CoNi nanoparticles for high-energy supercapacitors. Chemical Engineering Science, 2021, 240, 116649.	1.9	11
483	Electricity generation from water evaporation through highly conductive carbonized wood with abundant hydroxyls. Sustainable Energy and Fuels, 2022, 6, 2249-2255.	2.5	11
484	Intercalation of conducting poly(N-propane sulfonic acid aniline) in V2O5 xerogel. Journal of Applied Polymer Science, 2007, 103, 2569-2574.	1.3	10
485	Mg3N2-Ga: Nanoscale Semiconductor–Liquid Metal Heterojunctions inside Graphitic Carbon Nanotubes. Advanced Materials, 2007, 19, 1342-1346.	11.1	10
486	Electrostatic layer-by-layer self-assembly of PAMAM–CdS nanocomposites on MF microspheres. Materials Chemistry and Physics, 2007, 105, 315-319.	2.0	10

#	Article	IF	CITATIONS
487	Tin Oxide Nanowires Synthesized via Flat Flame Deposition: Structures and Formation Mechanism. Industrial & Engineering Chemistry Research, 2011, 50, 5584-5588.	1.8	10
488	Electrostatic Layer-by-Layer Assembly of Hierarchical Structure of Multi-Walled Carbon Nanotubes With Glass Fiber Cloth Reinforced Epoxy Composites. Journal of Macromolecular Science - Physics, 2014, 53, 673-682.	0.4	10
489	Au@TiO2 double-shelled octahedral nanocages with improved catalytic properties. Dalton Transactions, 2014, 43, 15111-15118.	1.6	10
490	Facile fabrication of silica–polymer–graphene collaborative nanostructure-based hybrid materials with high conductivity and robust mechanical performance. RSC Advances, 2015, 5, 25450-25456.	1.7	10
491	Largely enhanced transcrystalline formation and properties of polypropylene on the surface of glass fiber as induced by PEI-CNT and PEI-GO modification. Polymer, 2020, 186, 122025.	1.8	10
492	A general carbon monoxide-assisted strategy for synthesizing one-nanometer-thick Pt-based nanowires as effective electrocatalysts. Journal of Colloid and Interface Science, 2020, 572, 170-178.	5.0	10
493	Synthesis of Gramâ€5cale Ultrastable Mnâ€Doped 2D Perovskites for Lightâ€Emitting Diodes. Advanced Materials Interfaces, 2021, 8, 2002175.	1.9	10
494	BiPO ₄ â€Derived 2D Nanosheets for Efficient Electrocatalytic Reduction of CO ₂ to Liquid Fuel. Angewandte Chemie, 2021, 133, 7759-7763.	1.6	10
495	Tungsten and phosphate polyanion co-doping of Ni-ultrahigh cathodes greatly enhancing crystal structure and interface stability. Chinese Journal of Chemical Engineering, 2021, 37, 144-151.	1.7	10
496	Electrophoresis-microwave synthesis of S,N-doped graphene foam for high-performance supercapacitors. Journal of Materials Chemistry A, 2021, 9, 15766-15775.	5.2	10
497	Regulating Steric Hindrance in Redoxâ€Active Porous Organic Frameworks Achieves Enhanced Sodium Storage Performance. Small, 2022, 18, e2105927.	5.2	10
498	Co ₃ O ₄ Quantum Dot-Catalyzed Lithium Oxalate as a Capacity and Cycle-Life Enhancer in Lithium-Ion Full Cells. ACS Applied Energy Materials, 2022, 5, 2112-2120.	2.5	10
499	Enhancing Surface and Crystal Stability of the Ni-High NCA Cathode for High-Energy and Durable Lithium-Ion Batteries. Industrial & Engineering Chemistry Research, 2022, 61, 2817-2824.	1.8	10
500	Polyacrylic acid- <i>b</i> -polystyrene-passivated CsPbBr ₃ perovskite quantum dots with high photoluminescence quantum yield for light-emitting diodes. Chemical Communications, 2022, 58, 4235-4238.	2.2	10
501	Study on the mechanism of aluminum nitride synthesis by chemical vapor deposition. Materials Chemistry and Physics, 1997, 47, 273-278.	2.0	9
502	The process of coating on ultrafine particles by surface hydrolysis reaction in a fluidized bed reactor. Surface and Coatings Technology, 2000, 135, 14-17.	2.2	9
503	Preparation of TiO ₂ â€Coated Al ₂ O ₃ Particles by Chemical Vapor Deposition in a Rotary Reactor. Journal of the American Ceramic Society, 1999, 82, 2044-2048.	1.9	9
504	Fabrication of core–shell latex spheres with CdS/polyelectrolyte composite multilayers. Colloids and Surfaces A: Physicochemical and Engineering Aspects, 2005, 264, 215-218.	2.3	9

#	Article	IF	CITATIONS
505	Properties of CeO2-ZrO2 Solid Solution Supported on Si-Modified Alumina and Its Application in Pd Catalyst for Methane Combustion. Chinese Journal of Catalysis, 2008, 29, 1043-1050.	6.9	9
506	Template-free approach for hydrothermal fabrication of ZnO microspheres. Particuology, 2009, 7, 225-228.	2.0	9
507	Structure controlling and process scale-up in the fabrication of nanomaterials. Frontiers of Chemical Engineering in China, 2010, 4, 18-25.	0.6	9
508	Large-scale synthesis of hollow titania spheres via flame combustion. Particuology, 2011, 9, 632-636.	2.0	9
509	Study of the Preparation and Properties of PBT/Epoxy/SiO ₂ Nanocomposites. Journal of Macromolecular Science - Physics, 2011, 50, 967-974.	0.4	9
510	Fabrication of CuInS2–TiO2 composite fibers by using electrospinning coupled with solvothermal method. RSC Advances, 2012, 2, 4055.	1.7	9
511	Flexible Free-Standing Hierarchical Carbon-Coated CoP ₂ Nanosheets for High-Performance Lithium-Ion Batteries. ACS Applied Energy Materials, 2018, 1, 7253-7262.	2.5	9
512	Microscopic insights into the ion transport in graphene-based membranes with different interlayer spacing distributions. Chemical Engineering Science, 2020, 212, 115354.	1.9	9
513	Promoting the dispersibility of silica and interfacial strength of rubber/silica composites prepared by latex compounding. Journal of Applied Polymer Science, 2020, 137, 49526.	1.3	9
514	Nitrogen-doped carbon stabilized LiFe0.5Mn0.5PO4/rGO cathode materials for high-power Li-ion batteries. Chinese Journal of Chemical Engineering, 2020, 28, 1935-1940.	1.7	9
515	Flame process constructing CQDs/TiO2-C heterostructure with novel electron transfer channel between internal and external carbon species. Combustion and Flame, 2021, 228, 163-172.	2.8	9
516	Nanofiber-reinforced transparent, tough, and self-healing substrate for an electronic skin with damage detection and program-controlled autonomic repair. Nano Energy, 2022, 96, 107108.	8.2	9
517	The Effect of SnO2 on the Photocatalytic Activity of Aerosol-Made TiO2 Particles. Journal of Materials Synthesis and Processing, 1999, 7, 357-363.	0.3	8
518	The effect of pressure deformation on dielectric and conducting properties of silicone rubber/polypyrrole composites in the percolation threshold region. Smart Materials and Structures, 2005, 14, 949-952.	1.8	8
519	Fabrication and characterization of cerium-doped barium titanate inverse opal by sol–gel method. Journal of Solid State Chemistry, 2007, 180, 301-306.	1.4	8
520	Synthesis and Structural Characterization of Polyaniline/Mesoporous Carbon Nanocomposite. International Journal of Polymer Analysis and Characterization, 2008, 13, 25-36.	0.9	8
521	Synthesis and characterization of electrically conductive and fluorescent poly(N-[5-(8-hydroxyquinoline)methyl]aniline)/V2O5 xerogel hybrids. Synthetic Metals, 2009, 159, 366-371.	2.1	8
522	Nonisothermal Crystallization Behaviors of Poly(butylene terephthalate) Nucleated with Elastomer-Modified Nano-SiO ₂ , a Commercial Nucleating Agent (P250), and Talc. Journal of Macromolecular Science - Physics, 2010, 49, 514-527.	0.4	8

#	Article	IF	CITATIONS
523	Synthesis, Characterization and Electrochemical Capacitance of Urchin-Like Hierarchical Polyaniline Microspheres. Journal of Macromolecular Science - Physics, 2012, 51, 897-905.	0.4	8
524	A new fabrication method of uniformly distributed TiO2/CNTs composite film by in-situ chemical vapordeposition. Materials Letters, 2013, 96, 203-205.	1.3	8
525	Building radially oriented architecture by tailorable V2O5 nanoribbons toward enhanced lithium storage. Chemical Engineering Journal, 2016, 304, 194-200.	6.6	8
526	Revealing the Electrochemical Mechanism of Cationic/Anionic Redox on Li-Rich Layered Oxides via Controlling the Distribution of Primary Particle Size. ACS Applied Materials & Interfaces, 2019, 11, 25796-25803.	4.0	8
527	Scalable solid-phase synthesis of defect-rich graphene for oxygen reduction electrocatalysis. Green Energy and Environment, 2023, 8, 224-232.	4.7	8
528	Help nanorods "stand―on microsubstrate to form hierarchical ZnO nanorod-nanosheet architectures. CrystEngComm, 2011, 13, 4861.	1.3	7
529	Functional Carbon Nanotube/Mesoporous Carbon/MnO2Hybrid Network for High-Performance Supercapacitors. Journal of Nanomaterials, 2014, 2014, 1-6.	1.5	7
530	Fluxing template-assisted synthesis of sponge-like Fe2O3 microspheres toward efficient catalysis for CO oxidation. Applied Surface Science, 2018, 444, 763-771.	3.1	7
531	Carbon-loaded ultrafine fully crystalline phase palladium-based nanoalloy PdCoNi/C: facile synthesis and high activity for formic acid oxidation. Nanoscale, 2019, 11, 17334-17339.	2.8	7
532	Pt1.4Ni(100) Tetrapods with Enhanced Oxygen Reduction Reaction Activity. Catalysis Letters, 2021, 151, 212-220.	1.4	7
533	Operando generated copperâ€based catalyst enabling efficient electrosynthesis of 2,5â€bis(hydroxymethyl)furan. Fundamental Research, 2023, 3, 763-769.	1.6	7
534	Defect engineered SnO ₂ nanoparticles enable strong CO ₂ chemisorption to formate. Dalton Transactions, 2022, 51, 3512-3519.	1.6	7
535	Materials science communication effect of doped silicon on structure and magnetic properties of Î ³ -fe2o3 particles. Materials Chemistry and Physics, 1997, 51, 169-173.	2.0	6
536	Morphological structure of nanometer TiO2–Al2O3 composite powders synthesized in high temperature gas phase reactor. Chemical Engineering Journal, 2001, 84, 405-411.	6.6	6
537	Melt processable conducting poly(aniline-co-o-anisidine)/linear low-density polyethylene composites with ethylene-acrylic acid copolymer as compatibilizer. Journal of Applied Polymer Science, 2005, 98, 1511-1516.	1.3	6
538	Poly(anilineâ€coâ€oâ€anisidine)/Sulfonated Carbon Nanotubes Composites Prepared by Surface Adsorption Method. Journal of Macromolecular Science - Physics, 2008, 47, 743-753.	0.4	6
539	Synthesis and characterization of fluoreneâ€based rod–coil liquid crystal polymers. Polymers for Advanced Technologies, 2009, 20, 104-110.	1.6	6
540	Inhibited Transesterification of Poly(Butylene Terephthalate)/Poly(Ethylene Terephthalate)/SiO2 Nanocomposites by Two Processing Methods. Journal of Macromolecular Science - Physics, 2011, 50, 453-462.	0.4	6

#	Article	IF	CITATIONS
541	Batteries: 2D Monolayer MoS ₂ –Carbon Interoverlapped Superstructure: Engineering Ideal Atomic Interface for Lithium Ion Storage (Adv. Mater. 24/2015). Advanced Materials, 2015, 27, 3582-3582.	11.1	6
542	Thermally Induced Crystallization of High Quality CH ₃ NH ₃ PbI ₃ Film with Large Grains for Highly Efficient Perovskite Solar Cells. Chemistry - A European Journal, 2017, 23, 5658-5662.	1.7	6
543	Confined Co ₉ S ₈ into a defective carbon matrix as a bifunctional oxygen electrocatalyst for rechargeable zinc–air batteries. Catalysis Science and Technology, 2019, 9, 5757-5762.	2.1	6
544	Construction of hierarchical functional nanomaterials for energy conversion and storage. Particuology, 2020, 48, 34-47.	2.0	6
545	Inactive step-edge Pt atoms boost oxygen reduction reaction by activating adsorbed hydrogen atoms. Applied Surface Science, 2020, 504, 144434.	3.1	6
546	Engineering V ₂ O ₃ nanoarrays with abundant localized defects towards high-voltage aqueous supercapacitors. Journal of Materials Chemistry A, 2022, 10, 4825-4832.	5.2	6
547	Gas Diffusion Layer with a Regular Hydrophilic Structure Boosts the Power Density of Proton Exchange Membrane Fuel Cells via the Construction of Water Highways. ACS Applied Materials & Interfaces, 2022, 14, 17578-17584.	4.0	6
548	Fabrication of fluorescent hollow capsule with CdS–polyelectrolyte composite films. Materials Letters, 2006, 60, 3447-3450.	1.3	5
549	Silica Fibers with Triangular Cross Sections. Advanced Materials, 2006, 18, 1852-1856.	11.1	5
550	Nonisothermal crystallization behavior of a luminescent conjugated polymer, poly(9,9-dihexylfluorene-alt-2,5-didodecyloxybenzene). Polymer International, 2007, 56, 245-251.	1.6	5
551	Morphological Evolution from SnO ₂ Quantum Dots to Quantum Chains inside Channels of Mesoporous Spheres. Industrial & Engineering Chemistry Research, 2011, 50, 12542-12547.	1.8	5
552	Production of Flexible and Electrically Conductive Polyethylene–Carbon Nanotube Shish-Kebab Structures and Their Assembly into Thin Films. Industrial & Engineering Chemistry Research, 2012, 51, 5456-5460.	1.8	5
553	Lithium storage improvement from hierarchical double-shelled SnO2 hollow spheres. RSC Advances, 2014, 4, 10450-10453.	1.7	5
554	Preparation of Calcium Carbonate@Methyl Methacrylate Nanoparticles by Seeded-Dispersion Polymerization for High Performance Polyvinyl Chloride Nanocomposites. Industrial & Engineering Chemistry Research, 2015, 54, 7459-7464.	1.8	5
555	Plasmonic Au Decorated Singleâ€crystalâ€like <scp>TiO₂â€NaYF₄</scp> Mesoporous Microspheres for Enhanced Broadband Photocatalysis. Chinese Journal of Chemistry, 2017, 35, 949-956.	2.6	5
556	Evaluation of mixing performance for the industrial-scale radial multiple jets-in-crossflow mixing structure. Chemical Engineering and Processing: Process Intensification, 2019, 141, 107534.	1.8	5
557	Intrinsic Apyraseâ€Like Activity of Ceriumâ€Based Metal–Organic Frameworks (MOFs): Dephosphorylation of Adenosine Tri―and Diphosphate. Angewandte Chemie, 2020, 132, 23152-23156.	1.6	5
558	The synergetic effect of zinc phthalate and carboxymethyl cellulose – carbon nanotube of glass fibers surfaces on improving strength and toughness of polypropylene composite. Journal of Polymer Science, 2020, 58, 2022-2031.	2.0	5

#	Article	IF	CITATIONS
559	Surface covalent sulfur enriching Ni active sites of Ni ₃ S ₂ nanoparticles for efficient oxygen evolution. New Journal of Chemistry, 2021, 45, 3210-3214.	1.4	5
560	Highâ€ŧhermalâ€conduction and lowâ€cost composite originated from the tight packing structure of boron nitride sheets and binary alumina balls. Polymer Composites, 2021, 42, 3562-3571.	2.3	5
561	Visible-light Photocataltic Activity of Cr-doped TiO ₂ Nanoparticles Synthesized by Flame Spray Pyrolysis. Wuji Cailiao Xuebao/Journal of Inorganic Materials, 2009, 24, 661-665.	0.6	5
562	Confined construction of porous conductive framework Na3V2(PO4)3 nanocrystals and their ultrahigh rate and microtherm sodium storage performance. Chemical Engineering Science, 2022, 262, 117912.	1.9	5
563	Rheological Behavior of Aciculate Ultrafineα-FeOOH Particles under Alkaline Conditions. Journal of Solid State Chemistry, 1998, 141, 94-98.	1.4	4
564	Aerosol Spray Pyrolysis Synthesis of Porous Anatase TiO2 Microspheres with Tailored Photocatalytic Activity. Acta Metallurgica Sinica (English Letters), 2019, 32, 286-296.	1.5	4
565	The Proportion of Feâ€N X , N Doping Species and Fe 3 C to Oxygen Catalytic Activity in Coreâ€5hell Feâ€N/C Electrocatalyst. Chemistry - an Asian Journal, 2020, 15, 310-318.	1.7	4
566	Optimizing the catalytic activity of flameâ€sprayâ€pyrolyzed Pt/Fe ₂ O ₃ catalyst toward CO oxidation: Effect of fluorination and reduction. Nano Select, 2021, 2, 744-757.	1.9	4
567	<scp>Modified TiO₂</scp> @graphene oxide and montmorillonite synergistically enhanced multifunctional nanocomposite films. Polymer Composites, 2021, 42, 2511-2522.	2.3	4
568	Dechlorination-facilitated deprotonation of CoFe (Oxy)hydroxide catalysts under electrochemical oxygen evolution. Chemical Engineering Science, 2022, 252, 117270.	1.9	4
569	Electrophoreticâ€Driven In Situ Polymerization Depositing Highâ€Quality Perovskite Films for Photodetectors. Advanced Optical Materials, 2022, 10, .	3.6	4
570	Highly stable halide perovskites for photocatalysis <i>via</i> multi-dimensional structure design and <i>in situ</i> phase transition. Dalton Transactions, 2022, 51, 11316-11324.	1.6	4
571	Kinetics for Reduction of Aciculate Ultrafineα-Fe2O3Particles to Fe3O4Particles. Journal of Solid State Chemistry, 1997, 134, 248-252.	1.4	3
572	THE EFFECT OF POLYPYRROLE LOADING ON THE ELECTRORHEOLOGICAL PROPERTIES OF POLYPYRROLE/SBA-15 SUSPENSIONS. International Journal of Modern Physics B, 2007, 21, 5026-5032.	1.0	3
573	Preparation of poly(aniline-co-o-anisidine)-intercalated mesostructured manganese oxide composites by exchange reaction. Materials Research Bulletin, 2008, 43, 2145-2152.	2.7	3
574	On the Effect of Modifications to Montmorillonite for the Desulphurization of Synthetic Gasoline. Adsorption Science and Technology, 2011, 29, 197-210.	1.5	3
575	Effect of perfluoroalkylmethacrylate esterâ€ <i>grafted</i> â€linear lowâ€density polyethylene on the tribological property of polyoxymethylene–linear lowâ€density polyethylene composites. Polymer Engineering and Science, 2011, 51, 925-930.	1.5	3
576	Anisotropic photoelectric film assembled from mesoporous silica (MS)@CuO@FeS2 composite microspheres for improving photoelectric conversion. Journal of Colloid and Interface Science, 2013, 402, 50-57.	5.0	3

#	Article	IF	CITATIONS
577	TiO ₂ cement for high-performance dye-sensitized solar cells. RSC Advances, 2016, 6, 83802-83807.	1.7	3
578	Molten Salt-Assisted Growth of Perovskite Films with Submillimeter-Sized Grains. Industrial & Engineering Chemistry Research, 2017, 56, 524-529.	1.8	3
579	Multi-shelled LiMn1.95Co0.05O4 cages with a tunable Mn oxidation state for ultra-high lithium storage. New Journal of Chemistry, 2018, 42, 3953-3960.	1.4	3
580	Computational fluid dynamics simulation and experimental analysis of ultrafine powder suspension. Rare Metals, 2020, 39, 850-860.	3.6	3
581	Patterned catalyst layer boosts the performance of proton exchange membrane fuel cells by optimizing water management. Chinese Journal of Chemical Engineering, 2022, 44, 246-252.	1.7	3
582	New insights on ultrafast Na[solv]+ coinserted graphite driven by an electric field. Science China Materials, 2021, 64, 2967-2975.	3.5	3
583	Synthesis and Photocatalytic Properties of CNT/Fe-Ni/TiO ₂ by Fluidized Bed-chemical Vapor Deposition Method. Wuji Cailiao Xuebao/Journal of Inorganic Materials, 2012, 27, 33-37.	0.6	3
584	STRUCTURE AND PERPORMANCE OF POLYAMIDE 6 COMPOSITES REINFORCED BY GLASS FIBER COMPOUNDED WITH NANO-SiO ₂ OR CANBON NANOTUBES. Acta Polymerica Sinica, 2010, 00, 1333-1339.	0.0	3
585	DISPERSION AND CRYSTALLIZATION BEHAVIOR OF POLYPROPYLENE NANCOMPOSITES WITH $\langle I \rangle \hat{I}^2 \langle I \rangle$ NUCLEATING AGENT MODIFIED MULTIWALL CARBON NANOTUBES. Acta Polymerica Sinica, 2012, 011, 1374-1381.	0.0	3
586	Numerical simulation of flow field and residence time of nanoparticles in a 1000-ton industrial multi-jet combustion reactor. Chinese Journal of Chemical Engineering, 2022, 51, 86-99.	1.7	3
587	Bienzymatic glucose biosensor based on co-immobilization of glucose oxidase and horseradish peroxidase on gold nanoparticles-mesoporous silica matrix. , 2008, , .		2
588	Laminar mesoporous structure of modified montmorillonite clays and its formation mechanism. Journal Wuhan University of Technology, Materials Science Edition, 2012, 27, 321-327.	0.4	2
589	Research progress in materials-oriented chemical engineering in China. Reviews in Chemical Engineering, 2019, 35, 917-927.	2.3	2
590	Promoting reversible reaction of oxygen anions in cobalt-free lithium-rich layered oxides to improve their electrochemical performance. Applied Surface Science, 2021, 566, 150587.	3.1	2
591	Morphology and Structure of Carbon Nanocoils Synthesized <i>via</i> the Flame Combustion of Ethanol. Wuji Cailiao Xuebao/Journal of Inorganic Materials, 2008, 23, 1179-1183.	0.6	2
592	Preparation of TiO2Photocatalyst Dual-modified by Transition Metal Doping and Carbon Nanotube (CNT) Grafting. Acta Chimica Sinica, 2012, 70, 567.	0.5	2
593	Anode modified by BiFeO ₃ and application in resourceful treatment of salty organic wastewater. Micro and Nano Letters, 2019, 14, 683-687.	0.6	2
594	Regulating Steric Hindrance in Redoxâ€Active Porous Organic Frameworks Achieves Enhanced Sodium Storage Performance (Small 1/2022). Small, 2022, 18, 2270004.	5.2	2

#	Article	IF	CITATIONS
595	Boosting the efficiency of low-loaded Au on spongy Fe2O3 via interfacial ferric hydroxide for low-temperature CO oxidation. Materials Chemistry and Physics, 2022, 288, 126407.	2.0	2
596	HYDROGEN EVOLUTION OF WATER ELECTROLYSIS ASSISTED BY TITANIUM DIOXIDE AND NICKEL SULFIDE NANOCOMPOSITE. Modern Physics Letters B, 2013, 27, 1341015.	1.0	1
597	The formation of steady gas film on the inner wall of the radial multiple jets-in-crossflow reactor. Chemical Engineering and Processing: Process Intensification, 2019, 143, 107617.	1.8	1
598	Synergistic Effect of Hybrid Montmorillonite-reduced Graphene Oxide as Dual Filler for Improving the Mechanical Properties of PVA Composites by a One-step Procedure. Acta Polymerica Sinica, 2014, 014, 218-225.	0.0	1
599	Vacancy-mediated Interfacial Charge Transfer in Au-ZnO by Fe promoter for low-temperature CO oxidation Journal of Environmental Chemical Engineering, 2022, 10, 106651.	3.3	1
600	Self-assembly of ZnO Nanorod Bundles into Flowerlike Architectures by a Simple Hydrothermal Route. Wuji Cailiao Xuebao/Journal of Inorganic Materials, 2009, 24, 69-72.	0.6	1
601	Morphology and structure analyses of SnO2 thin film coated on Al2O3 ultrafine particles by gas phase reaction in fluidized bed. Journal of Shanghai University, 1999, 3, 62-65.	0.1	0
602	Enhanced hydrogen evolution process of water electrolysis assisted by photocatalysis. , 2011, , .		0
603	Analyzing of mixing performance determination factors for the structure of radial multiple jets-in-crossflow. Chinese Journal of Chemical Engineering, 2019, 27, 2626-2634.	1.7	0
604	Correction to "Integrated Reference Electrodes in Anion-Exchange-Membrane Electrolyzers: Impact of Stainless-Steel Gas-Diffusion Layers and Internal Mechanical Pressure― ACS Energy Letters, 2021, 6, 2238-2239.	8.8	0
605	PREPARATION OF PE/CNTs SHISH-KEBAB STRUCTURES USING SOLUTION CRYSTALLIZATION. Acta Polymerica Sinica, 2009, 009, 660-666.	0.0	0
606	Hydrothermal Synthesis and Characterization of Flowerlike YBO ₃ :Eu ³⁺ . Wuji Cailiao Xuebao/Journal of Inorganic Materials, 2009, 24, 1064-1068.	0.6	0
607	PREPARATION OF Ni@C/HDPE CONDUCTIVE COMPOSITES AND THEIR POSITIVE TEMPERATURE COEFFICIENT PERFORMANCE. Acta Polymerica Sinica, 2013, 013, 1159-1164.	0.0	0
608	NYLON 6 COMPOSITES REINFORCED WITH GLASS FIBER/ETHYLENE-MALEIC ANHYDRIDE COPOLYMER/MULTIWALLED CARBON NANOTUBE HYBRID STRUCTURES BY ELECTROSTATICAL ABSORPTION. Acta Polymerica Sinica, 2013, 013, 1262-1269.	0.0	0
609	Modelling study of particle formation process in the CVD reactor. , 1994, , 543-546.		0
610	Preparation of flame retardant glass fiber via emulsion impregnation and application in polyamide 6. Journal of Polymer Engineering, 2022, .	0.6	0